Department of Radio Science and Engineering

Periodic transmission lines for leaky-wave antenna applications at millimeter wavelengths

Tomas Zvolensky

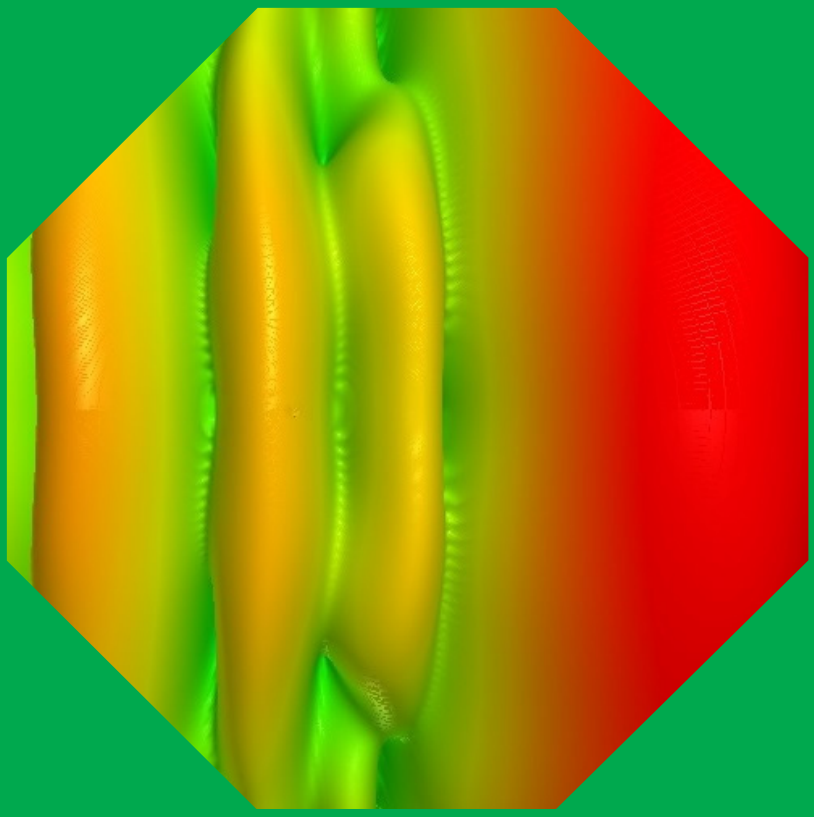

Aalto University

DOCTORAL DISSERTATIONS

Aalto University publication series
DOCTORAL DISSERTATIONS 190/2014

Periodic transmission lines for leaky-wave antenna applications at millimeter wavelengths

Tomas Zvolensky

A doctoral dissertation completed for the degree of Doctor of Science (Technology) to be defended, with the permission of the Aalto University School of Electrical Engineering, at a public examination held at the lecture hall S1 of the school on 12 December 2014 at 12.

Aalto University
School of Electrical Engineering
Department of Radio Science and Engineering

Supervising professor
Antti Räisänen

Thesis advisor
Professor Konstantin Simovski, D.Sc. (Tech) Juha Ala-Laurinaho, Dmitry Chicherin Ph.D.

Preliminary examiners
Professor Luis Enrique Garcia-Muñoz, Universidad Carlos III de Madrid, Spain
Simone Paulotto Ph.D., Head of Antenna Engineering and R&D at Maxtena, Inc.

Opponent
Professor Alessandro Galli, La Sapienza University of Rome, Italy

Aalto University publication series
DOCTORAL DISSERTATIONS 190/2014

ISBN 978-952-60-5975-4 (printed)
ISBN 978-952-60-5976-1 (pdf)
ISSN-L 1799-4934
ISSN 1799-4934 (printed)
ISSN 1799-4942 (pdf)
http://urn.fi/URN:ISBN:978-952-60-5976-1

Unigrafia Oy
Helsinki 2014

Finland

441 697
Printed matter

Author
Tomas Zvolensky

Name of the doctoral dissertation
Periodic transmission lines for leaky-wave antenna applications at millimeter wavelengths

Publisher School of Electrical Engineering

Unit Department of Radio Science and Engineering

Series Aalto University publication series DOCTORAL DISSERTATIONS 190/2014

Field of research Periodic transmission lines, leaky-wave antennas

Manuscript submitted 7 March 2014 **Date of the defence** 12 December 2014

Permission to publish granted (date) 21 October 2014 **Language** English

☐ **Monograph** ☒ **Article dissertation (summary + original articles)**

Abstract

This thesis focuses on planar leaky-wave antennas based on periodic transmission lines with resonant loads also called metamaterial transmission lines operating at millimeter waves. Planar transmission lines proved to be suitable for metamaterial transmission lines and are here investigated with regard to application as a leaky-wave antenna. Most of them can support backward wave propagation, but the ones with a ground plane provide better directive properties of the final leaky-wave structure.

Leaky-wave capability of a microstrip-based periodic transmission line is numerically verified as fit for electronic beam steering applications provided the technological readiness of MEMS technology. Experimental samples, with static MEMS capacitors used as a reactive load, centered at 77 GHz are fabricated in a clean room and measured using a probe station.
An alternative to a single antenna scanning system is designed and measured at 94 GHz. The antenna system is based on substrate integrated waveguide which was proved to be suitable and easy to fabricate technology in order to facilitate several antennas positioned next to each other to provide sufficient span of scanning angles.

A design method for periodic transmission lines based on planar lines is developed and verified. The most important contribution of this method resides in a linear approach to the design, ease of use, and span of applicability up to millimeter-wave range. The central steps of the design method are pre-compensation of parasitic impedances and periodicity pre-compensation. It is numerically and experimentally verified at 77 and 26 GHz, respectively. It is shown that the leaky-wave antenna designed by this method is capable of providing needed scanning angle range in order to be used in future automotive radar and sensor applications.

Eventually a detailed analysis of individual design steps is made resulting into a set of instructions and considerations when designing a periodic leaky-wave antenna or structure based on balanced one-dimensional periodic transmission line.

Keywords

ISBN (printed) 978-952-60-5975-4 **ISBN (pdf)** 978-952-60-5976-1

ISSN-L 1799-4934 **ISSN (printed)** 1799-4934 **ISSN (pdf)** 1799-4942

Location of publisher Helsinki **Location of printing** Helsinki **Year** 2014

Pages 134 **urn** http://urn.fi/URN:ISBN:978-952-60-5976-1

Preface

This thesis was carried out as a part of the studies towards a doctoral degree at the Department of Radio Science and Engineering at the Aalto University School of Electrical Engineering. As practically everything in life, also studying towards a doctoral degree is based on many conditions and behind these conditions are usually other people.

Therefore I would like to start with expressing deep gratitude to my supervisor Professor Antti Räisänen who accepted me for doctoral study program, and for his continuous support and guidance throughout the years spent at the Department. His fresh and open-minded approach to teaching and student guidance was a great inspiration for me. Many thanks go to my instructors Dr. Dmitri Chicherin and Dr. JuhaAla-Laurinaho who have been great support in research and practical matters. Professor Konstantin Simovski deserves my sincere gratitude for invaluable help during the research and writing periods. Moreover I am thankful to him for enabling my stay at Queen's University in Belfast as an exchange researcher. There I was guided by Associate Professor George Goussetis, Dr. Dimitry Zelenchuk and Dr. Neil Buchanan to whom I am grateful for accepting me to help them with their work. This thesis was partially supported by Tekes and the European Union FP7 program within the frame of projects SARFA and TUMESA, respectively, which included several industrial and academic partners to which I would like to express my gratitude, namely Mr. Mikael Sterner and Associate Professor Joachim Oberhammer from KTH – Royal Institute of Technology, Professor Ronan Sauleau of Université de Rennes, Mr. Jan Åberg of MicroComp Nordic and Dr. Frantz Bodereau of Autocruise S. A.

Next I would like to thank the colleagues, especially the Terahertz group for their constructive critics, suggestions, and ideas. Further thanks go to the service personnel of the Department of Radio Science for their support with practical issues. I highly appreciate and thank for the comments and observations of the pre-examiners.

Eventually I wish to thank my family – my parents and siblings for their support and understanding, my friends inside and outside Finland for creating great atmosphere and company, and my partner Ivana for her admirable patience and loving kindness.

Contents

List of publications

[I] T. Zvolensky, D. Chicherin, A. V. Räisänen, and C. Simovski, "Beam-steering MEMS-loaded antenna based on planar transmission lines," *Proceedings of the Fourth European Conference on Antennas and Propagation (EuCAP)*, 12-16 Apr. 2010.

[II] T. Zvolensky, D. Chicherin, A. Räisänen, and C. Simovski, "Leaky-wave regimes on MEMS-loaded transmission lines for mm-wave applications," *Progress in Electromagnetic Research M*, vol. 13, pp. 157-171, 2010.

[III] T. Zvolensky, D. Chicherin, A. Räisänen, and C. Simovski, "Leaky-wave antenna based on Microelectromechanical systems-loaded microstrip line," *IET Microwaves, Antennas & Propag*., vol. 5, pp. 357-363, 2010.

[IV] T. Zvolensky, D. Chicherin, A. Räisänen, C. Simovski, M. Sterner, J. Oberhammer, and H. Hakojärvi, "Leaky-wave antenna at 77 GHz," *Proceedings of the 41st European Microwave Conference*, pp. 1039-1042, October 2011.

[V] D. Zelenchuk, A. J. Martinez, T. Zvolensky, J. L. Gomez, N. Buchanan, G. Goussetis, and V. Fusco, "W-band substrate integrated waveguide technology for scanning antenna architectures," *Journal of Infrared, Millimeter and Terahertz Waves*, no. 34, pp. 127-139, January 2013.

[VI] T. Zvolensky, J. Ala-Laurinaho, A. Räisänen, and C. Simovski, "A systematic design method for CRLH periodic structures in the microwave to millimeter-wave range," *IEEE Trans. Antennas Propag*., vol. 62, no. 8, pp. 4153-4161, August 2014.

[VII] T. Zvolensky, J. Ala-Laurinaho, A. Räisänen, and C. Simovski, "Design aspects of finite periodic transmission lines based on planar structures," Submitted for publication in *European Conference on Antennas and Propagation 2015*, Lisbon, Portugal, 12-17 April 2015.

Contribution of the author

Publication [I]: "Leaky-wave regimes on MEMS-loaded transmission lines for mm-wave applications**"**

In this paper the author has developed a MATLAB code implementing the global optimization method used as a part of the design process of periodic leaky-wave antenna, developed numerical models and verified the beam-steering capability of coplanar waveguide-based structure. The author has prepared the manuscript with improvement provided by Prof. Antti Räisänen, Prof. Konstantin Simovski, and Dr. Dmitri Chicherin.

Publication [II]: "Beam-steering MEMS-loaded antenna based on planar transmission lines"

This paper is an extension of the analysis done in Publication I. The author carried out necessary design and computation of tested structures and prepared the manuscript, which was improved through the comments of Prof. Antti Räisänen, Prof. Konstantin Simovski, and Dr. Dmitri Chicherin.

Publication [III]: "Leaky-wave antenna based on micro-electromechanical systems-loaded microstrip line**"**

In this paper the author has designed a microstrip-based leaky-wave antenna with MEMS as an angle-steering component and carried out the numerical verification of the structure, and prepared the manuscript which was improved through the comments of Prof. Antti Räisänen, Prof. Konstantin Simovski, and Dr. Dmitri Chicherin.

Publication [IV]: "Leaky-wave antenna at 77 GHz**"**

Work in this paper extends the results of publication III. The author has re-designed the microstrip based leaky-wave antenna for fixed capacitance MEMS varactors with bonding wires, analyzed the measured data and prepared the manuscript except the chapter "Fabrication". M.Sc. Sterner manufactured the samples, Mr. Hakojärvi carried out the measurements, and Prof. Antti Räisänen, Prof. Konstantin Simovski, and Dr. Dmitri Chicherin helped to improve the manuscript.

Publication [V]: "W-band substrate integrated waveguide technology for scanning antenna architectures**"**

This paper is a result of collaboration with Dr. George Goussetis, Dr. Dimitry Zelenchuk, Dr. Alejandro Javier Martinez-Ros, Prof. Jose Luis Gomez-Tornero, Dr. David Linton, and Prof. Vincent Fusco. The author has

designed, analyzed and performed numerical simulations of coplanar waveguide to substrate integrated waveguide transitions as well as overall simulations of the antennas. Author has as well helped with measurements and manuscript preparation.

Publication [VI]: "A systematic design method for CRLH periodic structures in the microwave to millimeter-wave range**"**

In this paper the author has developed an easy to use methodology for design of periodic leaky-wave antennas based on planar transmission lines. This method was further verified by measurements of scattering parameters and radiation patterns carried out by the author. The manuscript was prepared by the author and improved through the comments of Prof. Antti Räisänen, Prof. Konstantin Simovski, and Dr. Juha Ala-Laurinaho.

Publication [VII]: "Design aspects of finite periodic transmission lines based on planar structures**"**

In this paper author analyzed various aspects of the design of periodic transmission lines and verified the fixed frequency beam-steering capability of leaky-wave antenna based on microstrip line. The author has carried out the analysis and prepared the manuscript. Prof. Antti Räisänen, Prof. Konstantin Simovski, and Dr. Juha Ala-Laurinaho helped to improve the paper with their comments.

List of abbreviations

CEM	Computational electromagnetics
CRLH	Composite right/left-handed
DC	Direct current
DRIE	Deep reactive ion etching
EM	Electromagnetic
FEM	Finite element method
HFSS	High frequency structure simulator
LH	Left-handed
LWA	Leaky-wave antenna
MEMS	Microelectromechanical systems
OPT	Optimized
PIN	P-type, intrinsic semiconductor, N-type junction
PN	P-type, N-type junction
PSO	Particle swarm optimization
PTL	Periodic transmission line
RF	Radio-frequency
RH	Right-handed
SIW	Substrate integrated waveguide
SRR	Split ring resonator
TE	Transverse electric
TL	Transmission line
TRM	Transverse resonance method
1-D	One-dimensional
2-D	Two-dimensional
3-D	Three-dimensional

List of symbols

A	Overlapping area of microstrip and membrane
A_T	Transmission matrix voltage coefficient
a	Size of the larger wall of waveguide
B	Magnetic flux density
B_T	Transmission matrix impedance
C_{End}	Open microstrip end capacitance
C_{ff}	Fringing capacitance
C_{Gap}	Microstrip gap capacitance
C_{PP}	Parallel plate capacitance
C_L	Left-handed capacitance
C_R	Right-handed capacitance
C_T	Transmission matrix admittance
D	Electric field density
D_T	Transmission matrix current coefficient
d	Via diameter
E	Electric field
$F(z)$	General field quantity
g	Height of a gap between microstrip and membrane
H	Magnetic field
h	Substrate thickness
I_n	Current at the gate of n^{th} cell
k	Wave number of loaded transmission line
k_o	Wave number in vacuum
k_n	Wave number of periodic structure
L_L	Left-handed inductance
L_R	Right-handed inductance
l	Line length
p	Period size
S_{11}	Input port reflection coefficient
S_{21}	Forward transmission coefficient
S_{12}	Reverse transmission coefficient
S_{22}	Output port reflection coefficient
V_n	Voltage at the gate of n^{th} cell
w_{eff}	Effective width of SIW
Z_o	Characteristic impedance
Z_B	Bloch impedance
α	Attenuation constant

β	Phase constant
γ	Complex propagation constant
ε, ε_r	Permittivity, relative permittivity
θ	Main beam radiation angle
μ	Permeability

1. Introduction

Metamaterials have spread over the scientific communities in many disciplines. Electrical engineering and in particular radio science is not an exception. Introduction of materials with negative permittivity and permeability brought about many novel applications, such as invisibility cloaks or superlens. This thesis focuses on planar leaky-wave antennas based on periodic transmission lines with resonant loads also called metamaterial transmission lines. Based on 1-D metamaterial concept, leaky-wave antennas are able to scan the main beam radiation from backward to forward directions with seamless transition over the broadside. Angle scanning capability is desired for smart antenna links, reconfigurable arrays, radar antennas etc.

In Chapter 2 the concepts of metamaterials, periodic structures and tuning elements are outlined with regard to the main principles and applications in terms of radio engineering. A model of MEMS developed and used as a part of the thesis work [I-IV, VI] is described and shown to provide a convenient tool for MEMS design.

Chapter 3 is dedicated to leaky-waves and antennas. Main classes of leaky-wave antennas are covered. A quasi-uniform scanning antenna system is introduced and experimentally verified [V]. Onward, composite right/left-handed (CRLH) leaky-wave antennas [I-III] are analyzed.

In Chapter 4 various transmission lines are examined [I] and a numerical analysis of leaky-wave antenna is performed in [II] and [III]. Design methods for periodic leaky-wave antennas are reviewed and an alternative design method for printed CRLH periodic transmission lines [VI] is introduced based on the Bloch analysis. The design approach is based on compensation of mutual couplings between the cells as additional parasitic inductances and capacitances added to a single unit cell.

Chapter 5 reports the results of experimental verification of the design method proposed and important design parameters such as electrical cell size, manufacturing inaccuracies and operation frequency are analyzed and design recommendations are given on this base.

Chapter 6 and 7 contain summaries of published manuscripts and concluding remarks together with an assessment of possible future research direction. Manuscripts I-VII can be found in the appendix.

1.1 Motivation, scope and objectives

The periodic structure considered in this work is in general an infinite transmission line periodically perturbed by discontinuities. These discontinuities store either electric or magnetic energy and therefore can be considered reactive elements. The transmission line can, in general, be any kind of transmission line used at microwave or millimeter-wave frequencies (e.g. rectangular waveguide, planar transmission line, or dielectric waveguide). Applications of periodic transmission lines are widely spread due to their natural pass-band and stop-band characteristics and used as filters, phase shifters, band-gap structures, antennas, or couplers.

The concept of metamaterials found its way into research and engineering life early in the last century, enabling novel ways to improve the functionality of devices and structures up to optical frequencies. Metamaterials describe a set of materials with properties not observed within natural materials. In particular, permittivity and permeability arising from the chemical and structural order can be under certain considerations simplified into the form to be used with conventional transmission lines.

One of the areas where metamaterials brought significant improvement to known practices and the design of structures is antenna design, including dimensional reduction, matching circuits, and new classes of antennas. Along with the improvement to their properties, introduction of metamaterials has also uncovered unexplored possibilities not considered feasible before. In particular, the long-researched topic of leaky-wave antennas, starting from the slotted rectangular waveguide and continuing with the micro-sized planar transmission lines, benefited significantly from the establishment of metamaterials. Due to their non-resonant nature and possibility to achieve high directivity with a small electrical size, leaky-wave antennas are especially suitable for applications where the compactness, easy fabrication, and fine angular resolution of the antenna are essential. This is the case with, e.g., automotive radars and its upcoming shift to the millimeter-wave frequency range. The advantage comes from the possibility to steer the main beam angle with numerous possible applications in intelligent sensors, scanning antenna arrays, or short range links.

Even though metamaterials are primarily defined as a bulk material with particular electrical properties, at microwave and millimeter-wave frequencies a 1-D structure is much easier to implement – this is the kind of

a structure to be dealt with throughout this thesis. The 1-D implementation is a straight forward process looking at metamaterial in light of transmission line and periodic structures theory. A 1-D metamaterial structure is obtained by periodically loading a transmission line with counterparts of its constitutive elements, inducing strongly dispersive properties of the formed structure. The period of the loading should be kept much smaller than the guided wavelength in which case the homogenization principle can be applied and the structure can be referred to as metamaterial. However, once the period is comparable to the guided wavelength, the structure can be called periodic, but not metamaterial. Keeping certain design principles in mind, this structure can behave as an antenna and, if tuned, or if the frequency of the feeding signal is swept, the direction of the main beam radiation can be controlled as well.

In this work the tuning elements considered are RF MEMS (Radio Frequency Micro-Electro-Mechanical-Systems) varactors and printed capacitors. The MEMS technology represents a promising option for this kind of application with its potentially superior properties such as low loss, high tunability (compared to semiconductor or ferroelectric devices) and tuning step small enough to be considered continuous opposed to step-wise.

Using commercially available simulators, a single unit cell of a periodic structure can be characterized. Because of neglected mutual coupling among the cells of resultant structure, the representation of the cascade based on this characterization yields inaccurate overall result. Design procedures of leaky-wave antennas have been described in many publications and vary significantly depending on the type of leaky-wave structure. Exact design methods for printed leaky-wave antennas are available and incorporate implementation of a specific-task full-wave code or extraction of complex transmission matrix roots. The latter combines usage of commercial software and correctly accounts for the mutual cell coupling providing a useful design tool.

The aim of this thesis is to investigate the design of leaky-wave antennas for the frequency range up to 100 GHz and for the electrical size of loading period varying from small to comparable to the guided wavelength. The expected outcome is a thorough design guide for the whole band with the minimum time spent on numerical optimization. Additional goal of this work is to verify the possibility to control the main beam of a metamaterial based leaky-wave antenna in the millimeter-wave range.

Since the development of microfabrication techniques, originating in the microelectronics industry, the fabrication of loaded planar lines – be it a simple structure from an engineering point of view – is rather unusual for microfabrication processes, and therefore challenging task, especially

considering MEMS varactors, which, unlike MEMS switches are yet to become a fully matured technology.

1.2 Scientific contribution of this work

The new scientific results achieved in this work are connected mainly to the leaky-wave antennas based on CRLH transmission lines. Several prototypes of MEMS loaded leaky-wave antennas and interdigital capacitor loaded antennas were fabricated to prove the usability of MEMS technology and novel methodology for the design of periodic transmission lines based on planar lines in general. Following points represent the contribution to the scientific knowledge:

1. Dispersive properties of various planar transmission lines are studied and shown suitable for leaky-wave antenna design in the range of millimeter-waves.
2. Analytical and numerical feasibility study of using MEMS capacitor as a tuning element for leaky-wave antennas for automotive radar applications is elaborated.
3. Analytical models and design procedure of distributed elements (such as MEMS capacitor, interdigital capacitor, and short microstrip section inductor) based on mixed analytical-numerical approach incorporating global optimization method is developed and verified.
4. A general method for design of periodic transmission lines based on planar lines is outlined. This method combines the advantages of presently used methods– simplicity of use, very good accuracy, and validity up to millimeter-wave frequencies with potential extension to even higher frequencies.
5. The general method for the design of periodic leaky-wave antennas with through-broadside scanning (or, balanced periodic transmission line) is numerically and experimentally verified at 77 and 26 GHz, respectively.
6. Design guidelines and considerations for periodic transmission lines are outlined and numerically studied with regard on the most important parameters – electrical size of the unit cell, frequency of operation, and fabrication tolerances.

2. Background

2.1 Metamaterials

Throughout the scientific and industrial world, materials have been considered to possess their properties within certain limits, discovered through the measurements of substances found in nature. The influence and response of materials to propagating electromagnetic waves are described by the inherent material parameters – permittivity and permeability, which themselves can be complex, and which have been traditionally confined to positive values. However, the realization of negative variations have been extensively studied in the past [1, 2], yielding artificially constructed materials, or metamaterials, which has spawned a new focus in the paradigm of electromagnetics and material research.

The topic of artificial materials that will be discussed throughout this thesis has been considered already in the last century [3], but has been practically implemented only at the beginning of this century. The idea was to have effectively homogeneous material with properties not found with natural materials. Since these materials are 'composed' of conventionally used materials, the unusual properties are achieved by the structural order and orientation of the constitutive parts. Here, the notion of effective homogeneity is important because it gives rise to the limitation of applicability of such materials. The limitation is mainly connected to the frequency range in which we can consider the composed material homogeneous, i.e. consider the material being based on uniform matter. The traditional limitation is commonly defined whereby the period between the particles is smaller than a quarter of the guided wavelength of the wave transmitted through the material.

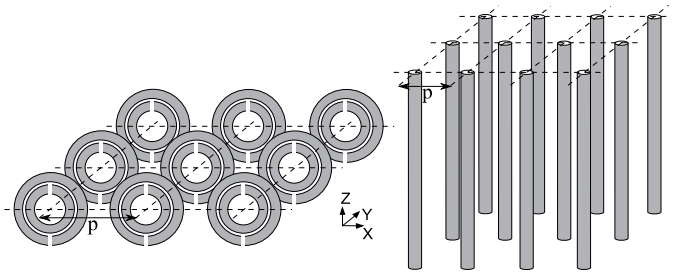

Figure 1 Particles of (left) negative μ media (split ring resonators), and (right) negative ε media, as suggested by Smith et al. [4].

Strictly speaking the quarter-wavelength limit is merely approximate and as such is not strictly defined.

Recent work [4] has experimentally proven the purely theoretical notion of backward-wave media in which the phase is propagating in the opposite direction to the energy propagation direction. The first backward-wave media were realized by combining a wire medium, which was studied in the 1960's [1], and a split-ring resonator (SRR), studied already in the 1950's [4, 5]. In [4], Smith et al. proposed and demonstrated this composite periodic medium (displayed in Fig. 1) having effectively negative permittivity and permeability at microwave frequencies.

Through backward-wave media, i.e. media exhibiting negative refraction, one can make a perfect lens [6] (principle sketch shown in Fig. 2), going beyond the square wavelength resolution limit due to cancellation of decaying evanescent waves, which are responsible for the focusing limit of conventional lens.

The concept of negative refraction was verified by Shelby et al. [7]. For the verification, a 2-D prism of SRRs and a wire media combination was fabricated, which demonstrated a measured negative refraction (scattering angle) of transmitted wave in microwave region.

Many papers on metamaterials followed, either conceptual or application oriented, together with number of textbooks. The textbooks focus mainly on the transmission line approach to metamaterials [8], analytical modeling of metamaterial structures [9] and present a compilation of scientific papers from different authors on the underlying physics and experimental verifications [10], or discuss the design and applications [11] emphasizing devices operating in visible or near-visible frequency range.

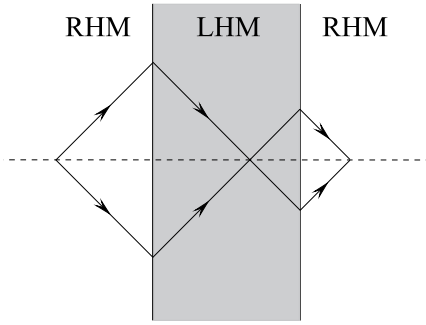

Figure 2 Sketch of a perfect lens based on left handed medium and negative refraction of rays impinging the boundary from the left hand side.

In this thesis the transmission line (TL) approach will be the pivotal theory used for the design and analysis of the leaky-wave antenna [12]. Since early papers describing metamaterials as a cascade of infinitesimally small circuits of lumped elements in one, two or three dimensions [5-7], numerous papers and monographs have been published [8, 13-17]. Examples of 1-D and 2-D metamaterial TLs are displayed in Fig. 3. A metamaterial transmission line is formed by loading conventional TL (right-handed TL: microstrip line, coplanar waveguide, rectangular waveguide, dielectric waveguide, etc.) by series capacitor, *C,* and shunt inductor, *L*, (together forming left-handed TL). This combination gives rise to highly dispersive behavior and the possibility of backward-wave propagation. Strictly speaking, the circuits in Fig. 3 do not represent the homogenization principle [18] since the RH TL does not appear in the form of series inductance and parallel capacitance, which would in this case be per-unit length quantities. This is common practice with the homogenization principle, but here the RH TL is in the form of sections of TL with certain wave impedance, Z_o, propagation constant, β, and length, l.

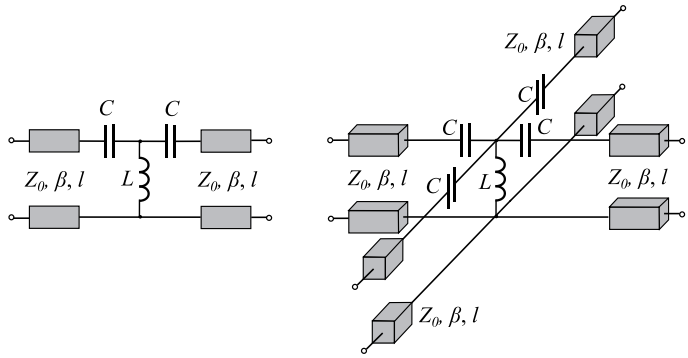

Figure 3 1-D and 2-D examples of lossless metamaterial transmission line composed of sections of a host transmission line and loaded with a LH circuit in order to obtain strongly dispersive characteristics.

2.2 Periodic structures

Speaking of material in general, we most frequently mean a bulk piece of uniform matter. This is of course a theoretical assumption since indeed real materials differ significantly from the models used. There are always inhomogeneities (at least on the atomic level) and statistic irregularities. Nevertheless, applying homogenization, averaging and mixing rules [8, 19] we obtain accurate means for describing the response of a realistic material to applied electromagnetic fields. From an engineering point of view, one of the first distinctions between materials has been the division into conductive and insulating materials. Starting with these quantities the knowledge of material properties has vastly increased in volume and diversity. Electromagnetic properties (and mixing rules) of materials are comprehensively described in [19] and will also be the main focus of this chapter.

Artificial bulk media (composites) have been a matter of research long before metamaterials were considered. The need to decrease the weight or dimensions of materials in certain applications [26] has been a natural driver for the development of artificial material research and engineering as a standalone branch. Artificial dielectrics [20] for light-weight microwave lenses and chiral materials for microwave radar absorbers [21] are just a few examples of artificial media applications.

Traditionally when thinking about certain medium, one imagines a matter composed of atoms ordered in more or less periodic fashion in a lattice. In connection to the electromagnetic characteristics of a given medium, if the period of the lattice is much smaller than the wavelength of the propagating wave, the macroscopic response can be described in terms of permittivity and permeability. Based on this fact one would automatically think that in order to create some artificial medium one would have to deal with atoms themselves. Looking at the size of the wavelength of micro or millimeter-waves, the situation is different. Order of centimeters or millimeters allows us to use known practices and materials arranged in a periodic way to obtain the macroscopic response that is similar to naturally occurring media, or as definitions of metamaterials [3, 6, 22-24] suggest, even properties not found with natural materials. In this fashion, parallel metallic plates have been used instead of a heavy dielectric lens for a horn antenna [25]. Metamaterials can be viewed as homogeneous materials and, roughly speaking, the composing particles can be seen as atoms on a microscopic scale. Nevertheless, depending on the frequency for which the metamaterial has been designed, the particles can even be seen by the naked eye, for instance at microwave frequencies, see Fig. 4.

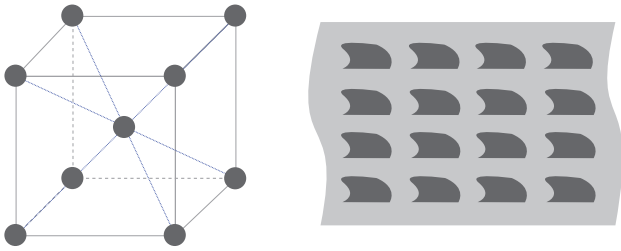

Figure 4 (left) Crystal cubic structure, and (right) metamaterial – periodic inclusions in a host medium.

Practical implementation of 3-D metamaterial structures is achievable through, for example, layered media stacked on top of each other with appropriate motives etched on their surface. However, this results in the desired properties being dependent on the polarization of the propagating wave. Negative refractive index media was initially achieved with structures composed of arranged split ring resonators (SRR), wire media (see Fig. 1) and so called fishnet structures at microwave frequencies up to the optical region [26-29]. In the optical range, 3-D structures have often one dimension considerably smaller than the wavelength even though the number of stacked layers can go up to ten [30].

Thus it is clear that the three-dimensionality of metamaterials can have a different meaning compared to what we usually imagine, with respect to the real structure. This can be reflected in the shape of a structure when the desired properties can be reached by using one layer of a medium instead of a bulk composed of many. Because the properties of metamaterials are strongly dependent on the distance of neighboring elements and layers, due to strong coupling effects, the flexibility and uncertainty of the design can increase. A metamaterial is considered 3-D when the addition of extra stacked layers does not change the polarization response of the metamaterial unit cell [30].

In the visible region the fabrication becomes challenging with regard to the required size of the unit cell and losses. At these frequencies metals exhibit large losses and become difficult to use as a building material for metamaterial structures. Dielectric spheres can be used instead. These posses negative permeability which is controlled by the size of the spheres [31]. Second order resonance of dielectric spheres is an electric dipole resonance [31] and it enables us to assemble a purely dielectric metamaterial by including spheres of different sizes into a host medium, provided that the size of the spheres is smaller than the wavelength of the applied field [32-35].

Fabrication processes stand for another chapter of bulk metamaterial production since the smallest features are usually sized in fraction of the wavelength. With growing frequency of operation, the fabrication processes

become more sophisticated and thus costly. Through microfabrication processes commonly used today, metamaterials can be composed by stacking the layers on top of each other using, for example, electron-beam lithography [35]. Although layer stacking is commonly used in practice, structures based on 3-D isotropic intra-connected unit cells can be realized by direct laser writing or directional evaporation technique [36, 37]. Vertical deposition of metal allows an almost arbitrary shape of the unit cell, making the conventional layered 3-D metamaterials truly bulk materials. Combining the metal and dielectric sheets, plasmonic waveguides are obtained, whereby the coupling of such waveguides can yield a material with negative refractive index [38].

2.3 Transmission line based metamaterials

In the previous chapter, metamaterials were considered in terms of a bulk piece of effectively isotropic matter composed of artificial particles that were smaller than the wavelength of the applied field. The analysis of these structures is mainly achieved through the application of Maxwell's equations. However, describing metamaterial layers in terms of the transmission line theory [39] is very convenient due to its relative simplicity and accuracy. Moreover, this approach reveals the link between periodically loaded transmission lines and regular metamaterials which obey to the same laws if we restrict our consideration by averaged electric and magnetic fields.

Impeccable advantages of transmission line theory compared to full wave analysis make it very useful particularly in engineering practice and design of metamaterial-based structures and periodically loaded transmission lines [8, 11, and 14]. In this case, the coupling of propagating waves has to be treated as a lumped source at the terminal of metamaterial transmission line, since the plane wave naturally does not couple to the transmission line without an appropriate transition, e.g. an antenna. Therefore the excitation has to be properly accounted for, which is in most applications done by default since the transmission line excitations are well-known and used [39]. On the other hand, with limitation on the wave polarization the free-space coupled transmission line metamaterial was demonstrated [40] through a transition layer similar to a horn antenna without vertical walls.

In this thesis we mainly work with 1-D metamaterial transmission lines. The 2-D and 3-D lines which are in essence an expansion of the 1-D structure are thus omitted from the analysis.

Description of any matter in terms of electromagnetic (EM) field interactions is done through two main parameters, permittivity ε and permeability μ. According to Maxwell's equations these relate the electric and

magnetic fields to the electric field density and magnetic flux density, respectively. Permittivity and permeability are, in general, tensors. Here we will mainly consider the EM wave to propagate in one direction, namely *z*. Thus, the constitutive relations can be written in the following way:

$$D = (\varepsilon_Z + j\varepsilon_Z)E \qquad B = (\mu_Z + j\mu_Z)H \tag{1}$$

Here, E is the electric field, D is the electric field density, H is the magnetic field, and B is the magnetic flux density. Transmission line theory allows us to express the permittivity and permeability in terms of impedances and admittances that compose a unit cell of a TL [39]:

$$\varepsilon_Z(\omega) = \frac{1}{\mathrm{p}}\left(\mathrm{C_R} - \frac{1}{\omega^2 \mathrm{L_L}}\right) \qquad \mu_Z(\omega) = \mathrm{p}\left(\mathrm{L_R} - \frac{1}{\omega^2 \mathrm{C_L}}\right) \tag{2}$$

Here p is the period size, and C_R, L_R, C_L and L_L are the per-unit cell parameters of the host TL and loading series capacitance and shunt inductance respectively. In general any kind of TL can be characterized in terms of cascaded infinitesimally small portions which are described by a series inductance, accounting for current flow, and a parallel capacitance, accounting for the voltage difference between conductors of the transmission line. The wave propagating through a TL composed of such cells is often called a Bloch wave which is typical for periodic crystal structures [8, 18, and 22].

Since the cell size – period p – is very small compared to the wavelength, the currents and voltages at the gates of each cell differ only by a complex propagation constant, this assumption is referred to as the Floquet theorem [8]. Another useful concept is the ABCD, or, transmission matrix which relates the currents $I_{n+1}=I_n e^{-\gamma p}$ and voltages $V_{n+1}=V_n e^{-\gamma p}$ at the gates of consecutive cells. For a two port circuit [39]:

$$\begin{bmatrix} V_{n+1} \\ I_{n+1} \end{bmatrix} = \begin{bmatrix} A_T & B_T \\ C_T & D_T \end{bmatrix} \begin{bmatrix} V_n \\ I_n \end{bmatrix} = \begin{bmatrix} V_n e^{-\gamma p} \\ I_n e^{-\gamma p} \end{bmatrix}. \tag{3}$$

The propagation constant, γ, describes the properties of the wave propagating through the periodic structure and can be obtained from (3) by solving the characteristic equation [39]:

$$A_T D_T + e^{2\gamma\gamma} - (A_T + D_T)e^{\gamma p} - B_T C_T = 0, \tag{4}$$

yielding [39]:

$$\cos \gamma p = \frac{A_T + D_T}{2}, \tag{5}$$

which can be used for extraction of the dispersion from simulation software after substituting the ABCD parameters for the scattering parameters:

$$\beta p = \cos^{-1}\left(\frac{1 - S_{11}S_{22} + S_{12}S_{21}}{2S_{21}}\right). \quad (6)$$

The impedance at the ports, which might be different from the impedance at any point within the cell, can be as well derived combining the Floquet theorem and ABCD matrix [8, 39]:

$$Z_B^{\pm} = \frac{\pm B_T Z_0}{\sqrt{A_T^2 - 1}}. \quad (7)$$

The sign of the solution depends on the direction of the traveling wave and the structure is assumed to be symmetric ($A_T = D_T$).

Transmission line metamaterials are widely used due to their favorable characteristics, mainly backward-wave propagation, low losses and ease of manufacture. Improved performance was observed with directional couplers [41, 42], phase shifters [43, 44], power dividers [45, 46], and antenna miniaturization [47].

2.4 Tunable elements at millimeter wavelengths and MEMS

Tuning of any device has two main functions. The first is to compensate for inaccuracies originating from fabrication errors. The second is to improve and extend the functionality of a device by changing the properties which are essential to its function. In this chapter we will concentrate on the latter in the band of microwave and millimeter-wave frequencies. Thin film, planar and waveguide technologies are dominating these bands and the tuning elements have either mechanical or electrical nature.

With waveguide technology the tuning is done through various kinds of metallic or dielectric screws, slits, wires, resonant irises, and diaphragms which by mechanical adjustment change its electrical properties, most often impedance. By loading the waveguide with a reactive load, the waveguide can become resonant, filter, or couple some of the energy of the wave. Examples of these tuning elements are shown in Fig. 5.

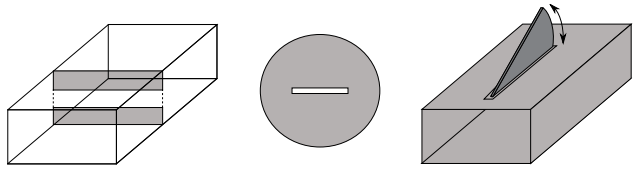

Figure 5 Waveguide tuning components: rectangular waveguide cross-section with inserted capacitive diaphragm, resonant aperture in circular waveguide and rectangular waveguide capacitive tuner (grey parts are metallic).

Planar technologies offer a broader variety of tuning elements due to easy integration of many components adopted from low frequency applications. Lumped elements used for tuning of circuits are in terms of technology

relatively easily transferable to the millimeter wavelength region. Semiconductor based components and micro-electromechanical systems (MEMS) are well developed devices, which can be used as electronically adjustable components.

In general, increasing the reverse voltage applied to a PN junction decreases its capacitance due to the increased width of the depletion region in the junction, which serves as a tuning element in many applications over a wide range of frequencies. Industrial demand for simpler filter networks without multiple switched filter branches has boosted the development of tuning elements, which has enabled reconfigurable filters requiring less space and material to be used. The tuning can be either step-wise, or continuous. For discrete tuning MEMS switches [48], CMOS [49], FET transistors [50, 51], HEMT transistors [52], liquid crystals [53], or PIN diodes [54] can be used, whereas for continuous tuning, MEMS capacitors, ferroelectric materials [55] or varactor diodes [56] can be employed.

Varactor diodes as tuning elements are widely used mainly up to X-band (8.2-12.4 GHz) frequencies. Low price makes them very attractive in this frequency region. In addition, with monolithic design higher frequency regions and a high degree of integration can be achieved. The insertion loss introduced by these switches depends on the number of diodes in the sequence and varies approximately on the order of a couple of decibels [57], which is not of great concern in the aforementioned frequency band since signal sources provide sufficient power levels.

Ferroelectric based capacitors, which can change the dielectric permittivity through an applied DC voltage, can be suitably incorporated into monolithic designs [58], but their high loss renders them unfavorable for wider use. Ferromagnetic materials are also reported to be used for tuning elements [59] but have not widely spread due to their low reconfiguration speed and higher cost.

MEMS devices can be used as a switch or as a variable capacitor [48, 60]. The main principle with MEMS is based on transformation of electrical or thermal energy into mechanical movement of the membrane. The main advantages, compared to solid state devices [49, 50, 52], or ferrite layers [61] are high isolation and quality factor, low weight and loss, small operational currents, and good compatibility with planar technology.

Switches can be cantilever or bridge type (see Fig. 6). Their implementation within low- or high- frequency applications is dependent on the contact type.

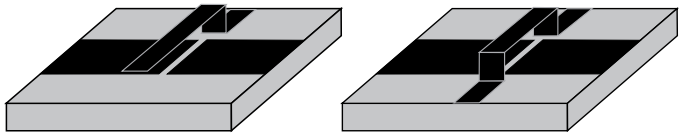

Figure 6 Cantilever (left), and bridge (right) - type of MEMS placed over a microstrip transmission line with a gap capacitor.

Low frequency switches can be metal-to-metal or resistive contact, whereas high frequency embodiments are usually capacitive, i.e. there is a small gap between the electrodes which are typically maintained in the 'on' state through a thin dielectric layer. Here we concentrate on radio frequency MEMS (RF MEMS). These are actuated by DC voltage to ensure electronic control [62, 63].

At low frequencies MEMS can be considered either purely capacitive (off state) or resistive (on state). Parasitic effects become non-negligible with increasing frequencies, resulting in more detailed equivalent circuit models, and their characterization. With growing frequency, besides the useful capacitance, part of the energy stored in the MEMS will be distributed between the parasitic inductances and capacitances. Since the parasitic components are in the order of useful capacitance, they will influence the performance of RF MEMS significantly.

The utilization of RF MEMS has found its place with many reconfigurable circuits like filters [64], phase shifters [65], impedance tuners [66], oscillators [67] and amplifiers [68]. Periodic transmission lines can be included in the filter category even though here they are mainly considered for leaky-wave antenna applications. Thus, by utilizing MEMS devices the main beam angle can be steered; for example, the series capacitor shown in Fig. 3 will be implemented as a steering MEMS element.

The following text will give a brief overview of the procedure of MEMS varactor design which was needed for successful implementation of a periodic TL. Due to the operation frequency of the proposed transmission lines being in the range of mm-waves, precise RF model which includes parasitic reactances was developed and verified. After an analytical model was found, a mixture of analytical and numerical optimization was used to optimize the performance of the MEMS [I, II, and III]. The computational electromagnetic model (CEM) and its equivalent circuit are shown in Fig. 7. The analytical design formula for MEMS parallel plate capacitance is [62]:

$$C_{PP} = \frac{\varepsilon_0 A}{g}, \tag{8}$$

where A is the overlapping area of membrane and microstrip, and g is the gap height between the membrane and microstrip line.

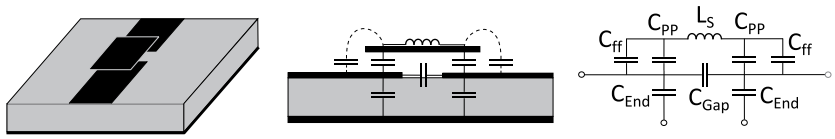

Figure 7 MEMS varactor model and its equivalent circuit: (left) angled view, (center) side view, and (right) substitute circuit. C_{ff} is the fringing capacitance, C_{PP} the parallel plate capacitance, C_{Gap} the microstrip gap capacitance, C_{End} microstrip open end capacitance and L_S series membrane inductance [VI].

The desired value of the capacitance was obtained with (8) and formulas for calculation of microstrip gap capacitance and open end capacitance [69]. The values of other parasitic components were obtained from basic transmission line equations [39]. A CEM model was created and simulated based on this analytical design. The results were exported to Matlab and compared with the results obtained by the analytical model. By means of particle swarm optimization (PSO) [70], the simulation results were fitted to the analytical data, which resulted into a set of corrections for the model parameters. This process was repeated until the desired capacitance values were achieved. This way we obtained a precise and fast method of MEMS device modeling and numerical characterization. An example of resultant comparison of fitted analytical model data and CEM model simulation results obtained from HFSS is shown in Fig. 8.

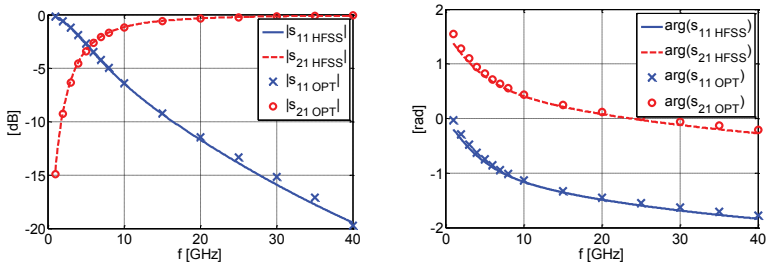

Figure 8 Comparison of magnitude and phase of fitted analytical model and results obtained from FEM simulation for MEMS varactor. Solid and dashed lines are HFSS simulation results and cross and circle lines are analytically fitted data [VI].

In [71-74], alternative approaches to MEMS modeling are introduced. The design method used in [I, II, and III] is mainly useful when scattering parameters [39] obtained from EM simulation software and Matlab (or any other suitable programming language) are available, which is advantageous during design of RF systems since the MEMS model does not have to be designed using separate tools.

Besides the guided wave applications mentioned, MEMS are widely used in antenna structures [75-78] with some initial studies also in the field of leaky-wave antennas [79]. Overview of LWAs steered using the alternative technologies mentioned can be found in [80-85].

3. Leaky-wave antennas

3.1 Leaky-waves

There are several types of waves which can propagate along open or closed wave-guiding structures [86]. In the case of a closed lossless structure the wave either propagates without attenuation (propagating field mode) or it is exponentially decaying along the structure (evanescent wave). In a layer of a lossless medium, there are continuous and discrete spectra of propagating waves. Quantitatively, wave numbers of such waves are either purely real or imaginary.

In a lossy structure the wave numbers are complex, having a real and imaginary part simultaneously, and the energy of the wave is being dissipated in metal, dielectric or radiation. This is the case for all realistic TLs especially at millimeter-waves. Waves with complex wave-numbers can propagate also along lossless guiding structures (e.g. waveguide with longitudinal slot), in which case we identify them as leaky-waves.

Leaky-wave is a type of complex wave which may be excited in open wave-guiding structures or closed ones with continual or periodic perturbation. A portion of a wave propagating along the transmission line is continuously radiating. In the leaky-wave regime radiation losses per unit length dominate over dissipative losses.

In order to excite a leaky-wave, a wave-guiding structure has to be perturbed by some kind of discontinuity. Using periodic perturbation with a period, p, we excite an infinite set of traveling wave components at each perturbation. These are referred to as space harmonics and can be expressed in terms of Floquet theorem, assuming the general time dependence as $e^{j\omega t}$ [87]:

$$F(z) = S(z)\mathrm{e}^{-\mathrm{j}k_0 z} \tag{9}$$

where $S(z) = S(z+p)$, $F(z)$ is a field quantity, k_o is a propagation wave number and $S(z)$ is a standing wave repeating its self every period p. Describing the standing wave in terms of Fourier series and inserting it into (9), we obtain [87]:

$$S(z) = \sum_{n=-\infty}^{+\infty} S_n e^{-jk_n z} \tag{10}$$

Wave number k_n is defined as periodic function $k_n = k_o + 2\pi n/p$ with $n = 0, \pm 1, \pm 2\ldots$ Components of the sum in (10) are in general infinite in number and decay very fast with increasing order of a given harmonic.

The k vs. β diagram has proved to be a very useful tool for the analysis of radiating structures. Separate space harmonics have their own dispersion curve, or, frequency dependent propagation constant, and can all together be plotted into a dispersion diagram. Mode coupling can occur between separate harmonics, meaning that the resultant dispersion diagram of a loaded line can be obtained by taking into account this coupling effect between the modes of an unloaded line. Depending on the sign of the group velocity, modes can couple in two ways – directional coupler type of coupling – i.e. both modes propagate in the considered frequency band dividing energy between each other. Second option is that a band-gap will occur, which prevents the wave propagation altogether [88]. Looking at Fig. 9 one can see that the coupling of unloaded transmission line space harmonics and the basic mode takes place always with modes with oppositely directed group velocities, resulting in a band-gap when $\beta p = 2\pi(n\text{-}1)$.

The kp vs. βp diagram for an open periodic structure is displayed in Fig. 10. Solutions for unilateral excitation are superimposed on the dispersion curves of the unloaded TL. If the line is inside the sequence of triangles the wave is fully bound to the guiding structure and is classified as a surface wave [86]. If the line passes through the shaded area, energy is continuously leaked into the free space. Such space harmonics radiate because the transversal wave number in the shaded region has real values, or it is higher than the free space wave number. This is illustrated in Fig. 11 where the complex leaky-wave propagates along a grounded slab. For this wave to radiate, the transversal wave number has to be real, which in this case is when $k_Y = (k^2 - k_Z^2)^{1/2}$ is real.

In Fig. 10 we can see that more space harmonics can radiate at the same time for $n = -1$ and $n = -2$, whereby the harmonics radiate simultaneously in the overlapping radiation frequency bands, B_{-1} and B_{-2}. This results in two beams with different angles of radiation in the overlapping frequency region. Depending on the application, this may be in fact desirable or not, the latter being for the case of scanning antennas.

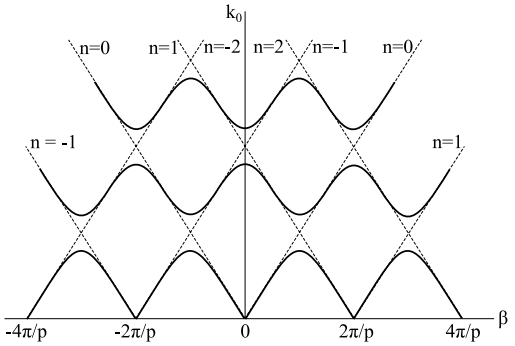

Figure 9 k_o vs. β diagram of a loaded TL. Dashed lines denote original space harmonics of an unloaded TL with infinitesimal loading spaced by $2\pi/p$, and full lines denote the dispersion curves after the mode coupling.

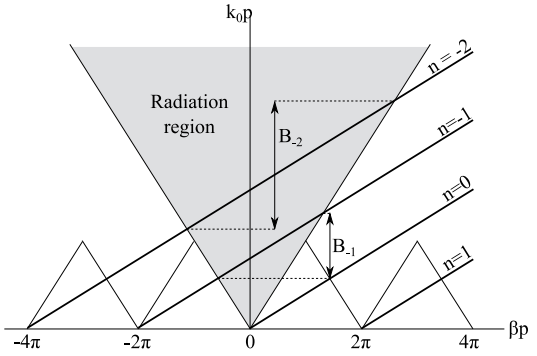

Figure 10 k_0p vs. βp diagram of an open periodically loaded TL with a radiation region denoted by the shaded area, and solutions of the dispersion for unilateral excitation. B_{-1} and B_{-2} are the bands in which the space harmonics are leaky.

The dispersion diagram in Fig. 10 is valid for printed periodic structures which do not support transverse surface waves. The structures mainly considered here, however – printed periodic 1-D structures based on grounded dielectric slab – do support surface waves due to finite transverse dimensions [89]. The radiation regions of the dispersion diagram thus change by including new regions of leakage into the surface wave modes.

In Fig. 12 such dispersion diagram is displayed. There are eight distinct regions of radiation. The ones with apostrophe identify radiation into the forward region and without into the backward region. The horizontal dotted line designates the cut-off frequency of TE_1 surface wave. The TM_0 surface wave has cut-off at DC [86].

The full line limits the fast wave region ($\beta < k_o$) as in Fig. 10. In regions A and A' leakage only into the TM_0 mode is present. Regions B and B' limit simultaneous propagation of TM_0 and TE_1 modes. In regions C, C', D and D' free space wave leakage occurs. Additionally, in C and C' the TM_0 surface wave propagates and in D and D' both TM_0 and TE_1 waves occur.

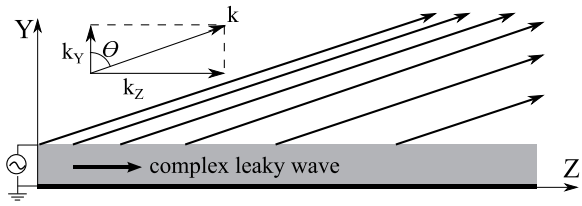

Figure 11 Leaky-wave propagation along a grounded dielectric slab. Energy is continuously radiated into the free-space along the direction of propagation Z under a given angle θ. The region of exponential growth means that the energy radiated increases in Y direction. The causality is not violated since the radiated energy is not growing to infinity but due to the specific position of the source it grows only until certain maximum value above which it is zero again.

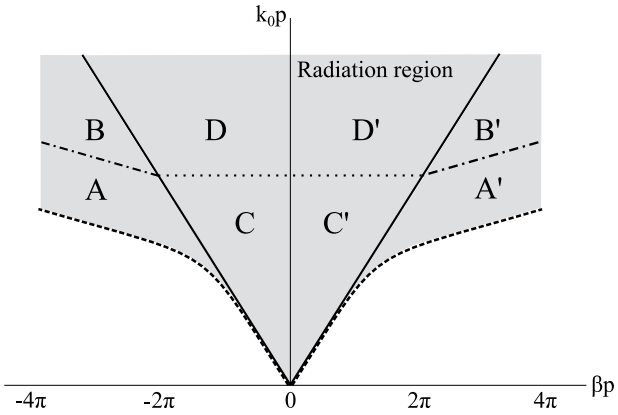

Figure 12 Dispersion diagram of a 1-D periodic transmission line based on grounded dielectric slab with finite transversal dimensions. Dashed lines define the propagation of a TM_0 surface wave, dashed-dotted lines of a TE_1 surface wave, and solid lines of a space wave [89].

This 'extended' dispersion diagram explains in detail possible radiating regions that may appear with periodic structures based on grounded dielectric slabs with finite dimensions in transverse direction (perpendicular to the direction of propagation of a guided wave) [89].

3.2 Uniform and quasi-uniform structures

The first leaky-wave structure was a rectangular waveguide with a longitudinal slit [90] on the narrow wall (Fig. 13). The first periodic leaky-wave antennas (LWA) were also based on rectangular waveguides and were meant to improve the properties of uniform structures by decreasing the leakage constant to obtain narrower main beam [91]. The main principle with waveguide antennas was to introduce a non-symmetrical perturbation which disturbs the currents flowing on the inner walls which causes the structure to radiate.

Such structures were studied around 1950 by Hansen [92], Rotman [93], and Hines and Upson [91]. The design principles developed have been used for many decades to follow.

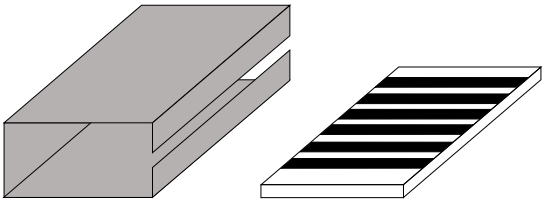

Figure 13 Examples of (left) uniform and (right) periodic leaky-wave antenna. In the uniform case, the cross-section of rectangular waveguide is the same along the structure. In the periodic case, a grounded dielectric slab with metal strips introduces periodic perturbations.

Much later, several other structures were investigated for leaky-waves, e.g. superstrate-substrate combination [94] and 2-D structures [95] based on partially reflecting surfaces.

With the advance of metamaterials [5-7], an increasing number of 1-D and 2-D structures were studied and verified [96-100]. More recently, substrate integrated waveguides allowed combining simple fabrication and high functionality of quasi-uniform leaky-wave structures [101-103].

The first important distinction with leaky-wave antennas was based on the structure profile, which can be uniform or periodic [90]. The transverse cross section of uniform structures is not changing along the structure. With periodic structures the profile is periodically modulated by some kind of discontinuity, example of which is shown in Fig. 13. The second important categorization is based on dimensionality of the structure – 1-D and 2-D leaky-wave antennas are recognized so far. The feeding method for the structure divides this type of antennas to end-fed structures and center-fed structures [104]. By feeding the structure either at one end or in the middle, we obtain one or two main radiation beams respectively, see Fig. 11 and Fig. 14.

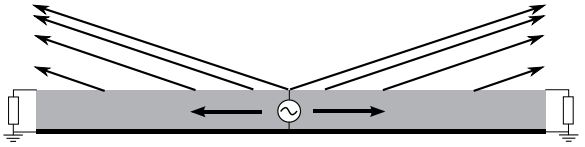

Figure 14 Center-fed structure loaded with matched load on both ends with two main radiation beams.

Quasi-uniform leaky-wave antenna structures can be treated as essentially uniform because the period of the perturbation is much smaller than the guided wavelength and the fundamental n = 0 space harmonic is radiating [105]. Therefore the periodicity is not directly involved with the radiation; see rectangular waveguide [87] or substrate integrated waveguide (SIW) structures [106]. Here, the basic guiding structure is a rectangular waveguide based on a metalized planar dielectric with closely spaced vias forming a

rectangular waveguide. The basic propagating mode is TE_{10} and the current responsible for radiation is written as:

$$I(z) = I_0 e^{-jk_z z} \tag{14}$$

where I_o is the amplitude and k_z is the complex propagation constant along the *Z* axis (see Fig. 11); this is essentially the same as (9) considering that the period, *p*, is very small which is the case for quasi-uniform structures.

The air filled waveguide is a standard example of uniform and quasi-uniform structures, conditioned by $p << a$. Since the basic TE_{10} mode of a waveguide is a fast-wave ($\beta < k_o$) it starts to radiate around the cutoff frequency up to the point when $\beta p = \pi$ when the n = -1 space harmonic becomes leaky and two radiation beams are observed. Design of a quasi-periodic leaky-wave structure will be described next, on the other hand, characteristics and design guidelines for uniform structures can be found in [12, 90, 107, and 108].

SIW structures can become leaky through various means, e.g., by introducing a periodic perturbation, uniform perturbation, or by decreasing the density of vias on one side of the waveguide [106, 109-111]. The sparse wall of vias effectively becomes a partially reflective surface and a portion of the energy from the propagating wave is continuously radiated [112]. Due to the simplicity of fabrication and ease of integration, SIW technology is a suitable option for fabrication of LWAs for millimeter wavelengths [113]. Long lasting interest in millimeter-wave technology is motivated by the scarcity of frequency bands in lower frequency regions. In addition to wider bandwidths, improved performance of many devices and availability of advanced technologies (e.g. thin film) further supports the development of systems operating in W-band, e.g. automotive radar [114], imaging sensors [115], or short range communication links [116].

Many applications in the millimeter-wave range require scanning the angle of the main beam, which can be achieved mechanically or electrically. In [V] we proposed antenna architecture based on a substrate integrated waveguide in order to cover a wide angular range at 94 GHz. The aim was to provide an alternative solution to structures with complicated feeding networks [117], volume intensive lenses or reflector antennas [118].

The usual challenge with leaky-wave antennas is to obtain a wide scanning range and since their fractional bandwidth is rather small a solution proposed here is to use three switched antennas to cover a range of angles from 5 to 55 degrees (measured clockwise from *Y* axis in *YZ* plane, see Fig. 11). The scanning of the radiation angle is based on the change of the propagation constant, which is achieved through varying the period, *p*, and width, *w*, as shown in Fig. 15. The effective width of a waveguide formed by SIW is given as [106]:

$$w_{eff} = w - 1.08\frac{d^2}{p} + 0.1\frac{d^2}{w}. \quad (15)$$

Based on the information on the equivalent waveguide width, the span of radiation angles can be obtained through (6). In this case, $\beta = (k^2 - k_c^2)^{1/2}$ where $k_c = \pi/(w_{eff}\sqrt{\varepsilon_r})$ [39].

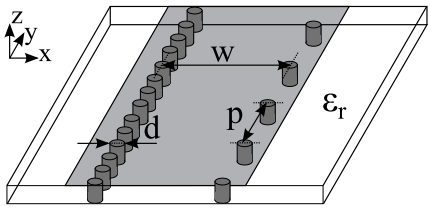

Figure 15 Substrate integrated waveguide with a sparse wall responsible for power leakage on the right side (metalized bottom not displayed).

By using the transverse resonance method [119] we can obtain the limit for the value of the relative permittivity of the substrate used for SIW fabrication in order to avoid total reflection inside the SIW. Satisfying this condition, the SIW is continuously leaking part of the energy of the propagating wave. From the condition of the substrate permittivity and cut-off frequency [120], the minimum operation frequency of the LWAs can be obtained. At the same time the number of antennas needed to cover a desired angular range can be derived provided that the scanning angle limits of the particular antennas are overlapping to seamlessly cover the whole range.

The scanning capability comparison is displayed in Fig. 16 for analytical and simulated results. It can be seen that approaching the broadside radiation (Θ = 0°) the performance deteriorates due to the approach to the cut-off frequency of the waveguide, which is dominated by strong dispersion. Resultant angular coverage of the system of three SIW antennas can be seen in Fig. 16.

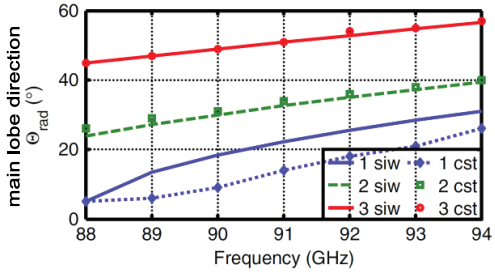

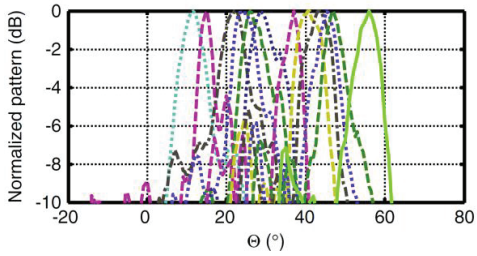

Figure 16 (top) Comparison of scanning ranges estimated by SIW formulas and by CST Microwave studio for three antennas, (bottom) measured patterns (in *YZ* plane in Fig. 15) of antenna system for the frequency range from 88 (cyan dotted line, $\Theta \approx 10°$) to 94 GHz (solid green line, $\Theta = 55°$) [V].

3.3 1-D periodic structures

The first periodic leaky-wave structures, i.e. rectangular waveguides, become leaky by introducing periodic circular holes along one of the walls [12, 90]. Since the holes are closely spaced, the principles of design for uniform structures can be used. The initially real propagation constant of the TE_{10} fundamental mode [39] $\beta = \sqrt{k_0^2 - (\pi/a)^2}$ is smaller than the free-space wave number which is the condition for the leaky-wave propagation constant to become real and thus radiate. The angle of radiation and leakage constant [12] are derived using $L/\lambda \approx 0.18 k_0/\alpha$ the stationary phase principle and under consideration of at least 90 % of power being radiated.

A convenient method to analyze waveguide based LWAs is the transverse resonance method (TRM) [39], which is in general used to obtain resonant frequencies of various cavities and wave numbers of complicated wave guiding structures, such as dielectric loaded rectangular waveguides or grounded dielectric slabs, etc. First, the equivalent circuit of transversally cut structure is drawn. Every discontinuity is substituted by impedance depending on its topology. Secondly, a reference plane is chosen and the circuit is solved for the condition of equality of the impedances when looking to either side of the plane [119]. The advantage of this method compared to a thorough EM analysis with applying boundary conditions is its simplicity. In [90] a thorough analysis of the most typical rectangular waveguide based LWAs has been done in terms of the TRM, yielding a summary of circuit parameters and attenuation constants needed to design such LWAs. The TRM can be used as well with planar structures, as shown in [119, 120], where a substrate integrated waveguide is used as the main wave guiding structure and leakage is achieved by decreasing the period p (see Fig. 15).

Opposed to uniform structures, periodic structures can easily radiate in both forward and backward directions and usually radiate from n = -1 space harmonic [121]. Looking closer at the propagation constant of a leaky-wave

propagating along the structure in Fig. 11, the difference between the forward wave and backward wave is following: since the imaginary part of

$$k^2 = (\beta_Z - j\alpha_Z)^2 + (\beta_Y + j\alpha_Y)^2 \tag{11}$$

is zero, then [87]

$$\alpha_Y = -\frac{\alpha_Z}{\beta_Y}\beta_Z\,, \tag{12}$$

and

$$\beta_Z = \beta_0 + \frac{2\pi n}{p} \tag{13}$$

where α_Z and β_Y are positive constants, and β_Z is a phase constant of a given space harmonic.

If $\beta_Z > 0$, α_Y is negative suggesting that the wave is amplified along the Y direction (Fig. 11). But in order for this solution to be physical, this amplification has to have a limit. If the leaky-wave was defined in the whole of space, the field strength would diverge to infinity in the transverse plane. In reality, the structure is finite and thus the growth of the amplitude continues only until a certain region above the structure, which is defined by the position of the source. Due to the exponential growth in the Y direction, this wave is called improper or non-spectral.

Comparatively, if $\beta_Z < 0$, α_Y is positive and the wave is exponentially decaying in the Y direction and is called proper or spectral. Together with the character of the wave, the sign of β_Z decides if the wave is forward or backward, i.e. if the angle of radiation θ is positive or negative, respectively (in YZ plane, see Fig. 11).

4. Design of 1-D periodic and CRLH leaky-wave structures

4.1 Introduction

Depending on the topology of the basic wave-guiding structure, application and dimensionality, the design procedures can differ significantly. Since the main types of TLs used for LWA design are rectangular waveguides, substrate integrated waveguides and various forms of planar transmission lines, the design and analysis methods are chosen accordingly. In the following section main design methods for periodic structures are reviewed and universal method developed as a part of the thesis is introduced.

To obtain the distributions of the fields associated with the waves propagating through planar periodic structures the functions of proportionality which connect the current density and vector potentials, or Green's functions, can be used. Here, the field on the aperture can be expressed as an inverse Fourier transform of Green's function. The electric component of the far field is equivalent to the Fourier transform of the aperture field and is mainly defined by the continuous part of the spectrum of the total field. The spectral Green's function has singularities in the form of poles and branch points. To identify whether the pole is significantly contributing to the leaky-wave field, the steepest descent method [122] of asymptotic evaluation can be used. It consists of transformation of the complex propagation constant plane to the cylindrical coordinate system, and deformation of the integration path to the steepest descent path. The position of the leaky-wave pole (in fast wave region or slow wave region) determines whether the contribution to the total field is significant or not [107, 108, 122].

First method for full-wave analysis of planar periodic structures is described in [123] and is based on a solution of mixed potential Green's functions, with exceptional accuracy. Application of the method presented in [123] requires a specific-task full-wave periodic program to account correctly for the coupling of neighboring cells, which is rather demanding. More references on the developments of full-wave methods and analysis of modal

properties of printed 1-D leaky-wave structures can be found in [123-129]. In [130] and [131] a computationally efficient approach to the calculation of mixed potential Green's functions is introduced, extending the work in [123] to arbitrarily shaped structures.

An approach based on the combination of numerical and analytical tools using the energy dissipated in a unit cell of periodic transmission lines, based on a microstrip line, has been introduced in [132]. Series and shunt modes of CRLH unit cells corresponding to the series and shunt resonances are used to extract the power dissipated within the structure for these two modes. Through the relation of these powers and circuit parameters of a given unit cell, its parameters are calculated. Comparison of numerical and analytical results (based on the data extracted from numerical EM solvers) showed ample agreement. Alternatively, even and odd-mode impedances can be used to describe behavior of arbitrary symmetric CRLH structures [133, 134].

Usual approximation used when simulating a single unit cell is, that the behavior of a single isolated unit cell is invariant when placed into a cascade. Because the discontinuities excite radiative fields, coupling between the neighboring cells can occur. To account for this coupling, a structure composed of a number of cells [121] or, an automatic routine implementing correct extraction of eigenvalues defining the wave numbers of a wave propagating along the periodic transmission line [135] can be used.

A MEMS controlled CRLH TL based phase shifter design procedure was introduced and experimentally validated in [71, 136, 137]. The procedure in [71] is based on numerical extraction of the parameters of the cell and optimization on the circuit level with iterative steps. The experimental validation is focused on one cell structure, its phase shifting ability, and was not expanded to periodic TLs.

CRLH TL based leaky-wave antennas, which radiate from n = 0 space harmonic have the advantage of absence of so called 'open-stopband' which is a well known issue with conventional leaky-wave antennas and waveguide arrays [12, 89], i.e. antennas radiating mainly from n = -1 space harmonic [12, 126]. Nevertheless, recently, a conventional leaky-wave antenna radiating from the n = 0 space harmonic was demonstrated [138]. The problem of open-stopband has been addressed [139] and finally eliminated [140, 141] by designing a suitable matching network, through which the Bloch impedance of each cell is matched to the impedance of the host TL at the broadside frequency assuring a flat response of Bloch impedance and antenna gain.

For many application oriented designs of periodic TLs the transmission line theory based approach is convenient due to its ease of use and its accurate description of the fundamental physics of metamaterials. The generally

accepted limitation to the application of the concept of effective homogeneity is that the size of the unit cell should be at most a quarter of a guided wavelength [8, 10, 14, and 16]. Exceeding this limit, the amplitude and phase variation of the fields over the cell length becomes significant. As mentioned in Chapter 2, the homogenization principle is built on substitution of the small sections of host TL by series inductor and shunt capacitor since the voltages and currents are quasi-stationary in this region. Loading the TL by series capacitor and shunt inductor, series and shunt resonant circuits are formed with different resonant frequencies in general. Further on, we will consider mainly the case when these frequencies are equal or the so-called balanced case [8, 16, and 17] being important for application in through-broadside scanning leaky-wave antennas. The properties of a balanced CRLH TL are extensively described in [8, 14, and 18].

Being strongly application oriented, the generally used design procedure for periodically loaded TLs in [8] starts with a choice of substrate and the dimensions of the chosen TL type. The per-unit length capacitance and inductance can be determined [39, 69] based on the cell size p. From the equations for resonance frequency for series and shunt circuits, and having chosen the center frequency for the TL, we obtain the values of series capacitance and shunt inductance needed to balance the unit cell. Using distributed elements to realize the capacitance and inductance, after the initial estimate of their values and their parasitic components, their separate full-wave simulations are performed. From these simulations the parasitic components are calculated based on derivatives of the impedance and admittance matrices at the extraction frequency and recursively corrected until sufficient accuracy is reached. Cascading the required number of cells, the periodic TL design is completed.

All the methods mentioned in this section have their advantages and disadvantages. After introducing the method developed as a part of this thesis in the next two sections, a comparison of the methods introduced will be presented.

4.2 Unit cell design

The design methods reviewed vary in accuracy, numerical and analytical demands, and the span of applicability. The algorithm proposed and verified herein is relying on the TL theory approach for initial design, and follows the rules for the design of 1-D periodic TLs based on planar lines. Emphasis with this method was put mainly on its ease of use, efficiency and universality.

In [I] a set of planar TLs (see Fig. 17) was investigated to verify the dispersive properties of unit cells based on these TLs and to establish which

structures are suitable to achieve a fan-shaped beam emanating from a LWA based on a given TL design. Based on the observation of the dispersion curves and Bloch impedance, all of the structures investigated were found to be suitable for the LWA application, since all dispersion curves indicated propagation constants that exhibited a band in which their values are below that of the free space propagation constant, with forward and backward wave regions with seamless transition.

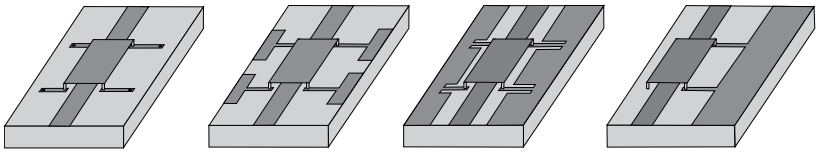

Figure 17 Investigated structures for application in LWAs, from the left – microstrip, microstrip with capacitive grounding, coplanar waveguide, and coupled stripes line [I].

The radiation properties of these structures were studied in [I] and [II] where the structures were loaded with MEMS varactors as series capacitors and short microstrip lines as shunt inductors. It was found that the shape of the radiation patterns most often resembles the distribution of the field of the basic propagating mode, and that structures without a ground plane radiate a portion of energy above and below the plane of the substrate, which is undesirable for application with LWAs. Therefore, coplanar waveguide and coupled strips lines were not further investigated.

In [III] the properties of microstrip based LWAs were investigated closely with an emphasis on the MEMS implementation and the resulting verification of scanning capability of the antenna when sweeping the capacitance of the MEMS. The dispersion curves for different MEMS capacitances are displayed in Fig. 18 together with the dependence of the scanning angle on the MEMS capacitance for the simulated and analytical case.

In [IV] a structure based on a microstrip line loaded with MEMS capacitors is designed, fabricated, and measured (measurement results shown in Chapter 5). The shunt inductance had to be increased due to the bonding wires which ensure a connection of the inductors to the ground plane, see Fig. 19.

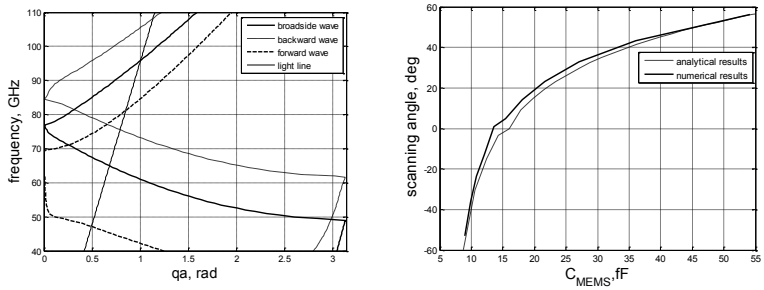

Figure 18 (left) Example of dispersion curves (center frequency 77 GHz) for three different MEMS capacitances. Comparison of analytical and numerical results (right) of scanning angle vs. MEMS capacitance dependence [III].

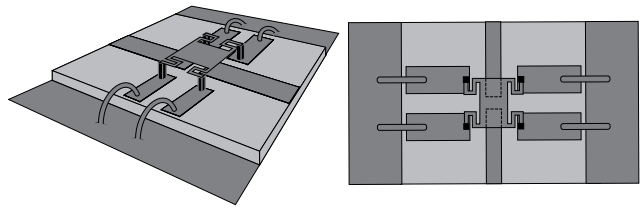

Figure 19 (left) Isometric and (right) top view on a unit cell based on a mircostrip line loaded with series MEMS capacitor and four shunt inductors grounded through bonding wires, which add to the total inductance [IV].

At this point, we will continue with the description of the design method from the basics in order to gain an overall perspective. It is a convention to start the design of periodic metamaterial transmission lines with the design of a unit cell comprising the resultant structure. The transmission line model in the simplest case includes components of a host transmission line, i.e. series inductance and shunt capacitance and the load of the transmission line – series capacitor and shunt inductor (see Fig. 20).

Due to the load, the transmission line becomes strongly dispersive [11]. Keeping the condition for the balanced state, the dispersion diagram typically exhibits a periodic region where the propagation constant of the loaded transmission line is smaller than in free-space, and the band gap (a region of frequencies where the wave constant drops to zero) bandwidth tends to zero. If the balance of the structure is not kept, the band gap, which corresponds to a standing wave, appears, whereby the transmission becomes zero and the reflection unitary, in this frequency region.

The precision of the design procedure used in [8] decreases with increasing center frequency. The higher the frequency, the more the parasitic components influence the overall performance of the unit cell. Approach of the analytical design, with a separate loading design and numerical optimization, works quite well at low frequencies (up to around X band), where the parasitic components are much smaller compared to the useful ones.

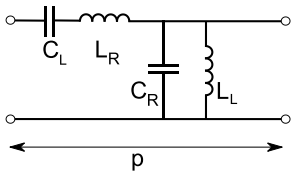

Figure 20 Simplified model of a CRLH TL unit cell, C_R and L_R are the parasitic components of the host TL, C_L and L_L are the loading elements, and p is the period size.

Increasing the frequency, the values of useful reactances have to decrease and thus the structure is increasingly influenced by parasitic components of the complex impedances of the distributed elements. After the analytical design, numerical simulations are usually required in order to verify the functionality of the cell before cascading (to obtain a periodic TL) and fabrication. At a few gigahertz the time spent on numerical simulations and optimization is relatively short. However, increasing the frequency the optimization time becomes significant. Thus, if we want to avoid excessive numerical optimization, the approach to the design has to be modified.

The modification comes from including the parasitic components into the model of the unit cell at the beginning of the procedure and compensating for the periodicity of the final structure. The equivalent circuit model of the cell naturally depends strongly on the technology used. Therefore, no universal model can be used despite the fact that they may often be quite similar. In our example we used interdigital capacitors, MEMS capacitors, and a short stub for the inductor as loading elements of the microstrip line. Similar procedure is used as with the MEMS capacitor in Chapter 2.4 with the difference that we consider the whole unit cell as an entity to be optimized. Another factor is coupling of the evanescent fields excited at the discontinuities, which couple with each other and further complicates the design of the unit cell.

To show the performance of the modified method, the design and validation of a unit cell at a center frequency of 26 GHz and 77 GHz will be reviewed based on [VI]. Obtaining the capacitance and inductance values from the balanced state condition (provided that the parameters of host transmission line and center frequency are fixed), the design of the loading elements has to be performed separately as suggested in [8]. For the short TL section inductor the same procedure can be used as for the MEMS (or interdigital) capacitor design using corresponding model. The number of numerical/analytical iterations is small if the analytical model corresponds to the actual distribution of energy in the unit cell structure.

The likelihood of the band gap occurrence (once analyzing the whole unit cell composed of separately designed loading elements) is increasing with increasing center frequency, even though we can extract the parameters of the loading with reasonable accuracy. The band gap appears due to the finite

precision of this method and mainly due to the coupling of evanescent fields excited at the series capacitor and shunt inductor. Mutual position of the loading within the unit cell is vital to this coupling effect [VII]. It was found by systematic testing that there is an optimal position of the capacitor and inductor for which the band gap is very small. This position is a subject to some optimization, but as the period size is always a fraction of the guided wavelength, time spent on this task is negligible.

4.3 Universal design method for CRLH periodic TL and leaky-wave antennas

The final dimensions of the balanced unit cell will, for most practical structures, differ from the ones obtained by analytical formulas. With the unit cell balanced, the common practice is to cascade the desired number of cells to obtain a periodic TL, leaky-wave antenna, phase shifter, patch antenna, etc.

At low frequencies the cascaded structure is close to the balanced state due to small influence of parasitic components and coupling, and a few iterations of numerical optimization are required to obtain well balanced structures, even though the iterative steps at this point may take considerable time depending on the number of cells in the cascade.

An increasing center frequency gives rise to intra-cell coupling of the distributed loading elements. In addition, inter-cell coupling influences the performance of the structure significantly. More precisely, by adding more cells into the cascade, the balance of the structure increasingly deteriorates, which results in a modified band gap that could be zero for the one cell case but differs with each added cell. The most significant difference is evident with the first additional cell – typically the band gap grows twenty five times (with center frequency being 77 GHz) and keeps growing, see Fig. 21.

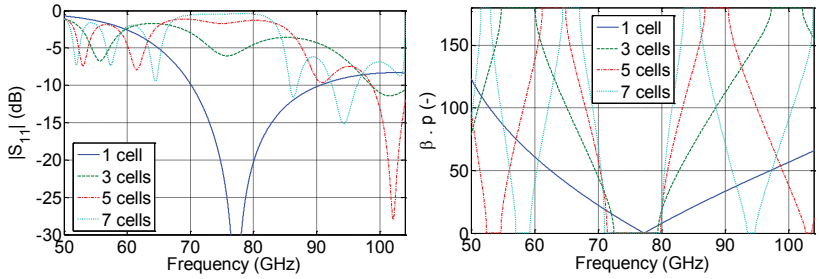

Figure 21 (left) Scattering parameters, and (right) dispersion diagram for structures with increasing number of cells, based on a cell balanced at 77 GHz with constant dimensions. Deterioration of the balanced state can be observed with each increase in cell number.

Theoretically each cell couples to every other cell in the whole structure. The closer the cells are, the stronger the coupling. At the same time, there is

a limit to the band gap growth since the contribution of distant cells is negligible compared to the ones in the vicinity of the observed cell.

The limit for this coupling has been found to be approximately fifteen cells [VI] with planar structures. Authors in [121] and [142] found this limit to be twelve and six respectively. In [121] a Bloch wave analysis was used to compare the full-wave analysis based on a solution of Green's function of a single unit cell and found the number of cells required to approach the precision of the full-wave method was at least twelve.

In [142] an extraction method based on the derivatives of impedances from the equivalent circuit model was used and found that at least six unit cells were required to obtain an approximation with sufficient precision (for lossless structure, two or three cells are enough). Both of these methods concentrate on the analysis of periodic TLs which yield the characterization of the unit cells and its components. This information may be useful for iterative design procedures, i.e. after designing the unit cell and simulating the corresponding properties using full-wave numerical software solutions, one can extract the values of cells' constituents and correct them accordingly, reiterating in order to obtain the cascade of the desired number of cells. Due to the aforementioned inter-cell coupling, the cascade of individually balanced (and identical) unit cells will result in an increased band-gap size with each added cell.

Analytically, this band-gap growth can be attributed to increasing and/or decreasing the values of the loading elements. Having the transfer function of the equivalent circuit model of our cell, a pair of dimensionless coefficients can be derived. Multiplying the values of L_L and C_L by these coefficients we obtain a unit cell whose band-gap is identical to the one observed with the cascades in Fig. 21. Examples of these coefficients are illustrated in Fig. 22 for particular periodic TL designs.

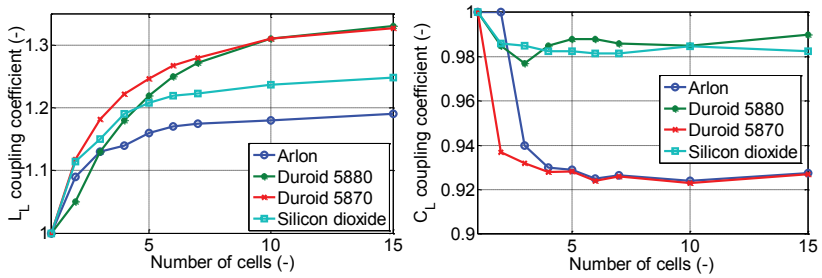

Figure 22 Coupling coefficient examples for various substrates and capacitor dielectrics. For the C_L coefficient, the blue and red traces represent the air dielectric and the rest represent Silicon dioxide as the MEMS dielectric (legend assigned dielectric is the carrier dielectric of the whole structure). The data points (crosses, circles, and squares) are fit by linear curves [VI].

By inverting this procedure, i.e. by multiplying the values of L_L and C_L by the inverse of the coupling coefficients we decrease the value of L_L and increase

C_L, thus un-balancing the unit cell. However, the corresponding cascade with the chosen number of cells will be balanced. This is because the coupling of parasitic fields between the cells will compensate for the band-gap which was created for the one-cell structure. An example of comparison of analytically obtained and actual resultant coefficients is displayed in Fig. 23. Solid agreement can be observed with the inductive coefficient.

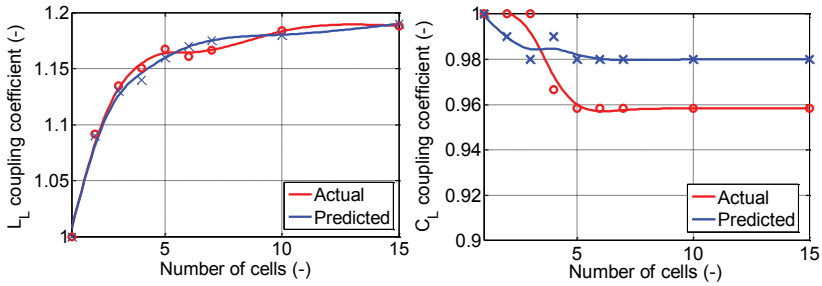

Figure 23 Comparison of analytically predicted and actual (based on full wave simulation) coupling coefficients. The data points (crosses and circles) are fit by polynomial curves [VI].

The capacitive coefficient is more erroneous, however, observing the scale of the error (in the order of 0.02) we can conclude that the analytical prediction of both coupling coefficients is precise. Applying this method, we obtained a series of cascades each of which is balanced around the center frequency with almost zero band-gap – see Fig. 24.

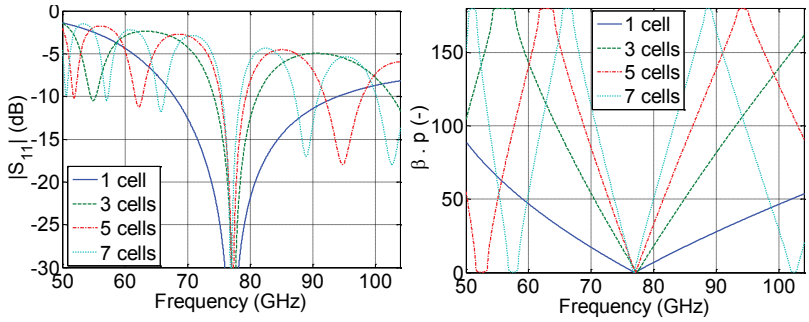

Figure 24 (left) Scattering parameters and (right) dispersion diagram of structures with increasing number of cells based on a cell balanced at 77 GHz with adjusted dimensions. Balanced state can be observed with all the cascades.

It is obvious from Fig. 24 that the method used for the design of periodic TLs proposed herein is efficient, fast, and easy to use. To the best of author's knowledge this is the first method which describes, in such detail, the design of periodic transmission lines based on planar lines. It can be summarized into the following design sequence:

1. Using formulas for a balanced TL [I, II, III], and arbitrarily chosen substrate, center frequency, and unit cell size, we obtain the values of C_L, L_L, C_R and L_L. Separate the design of series capacitor and shunt inductors according to Chapter 2.4.

2. Compensate for parasitic capacitances and inductances depending on the center frequency of periodic TL. For frequencies close to 100 GHz this step is crucial. For frequencies closer to DC the parasitic components are very small and thus the compensation is less critical and can be included in final optimization of the structure.
3. Compensate for inter-cell coupling by applying the coefficient multiplication for the corresponding desired number of cells. Similar consideration of operating frequency should be taken into account as in step 2.

The design procedure is thoroughly described in [VI] with detailed description and analysis of each step.

In Table I on the following page, a comparison of design methods for periodic TLs and leaky-wave antennas combined is presented. The method proposed here is named 'modified CRLH' and is mainly advantageous for planar periodic TLs with arbitrary metallization using mainly commercially available simulation software packages.

Table I [page 47] Comparison of various methods for designing periodic TLs and leaky-wave antennas.

method	precision	complexity	time demands	application area
GF solution [119, 130]	exact	high	moderate [119], low [130]	wide
Truncated structures [135]	high	moderate	moderate	planar PTL
TRM [75, 76]	very high	moderate	low	mainly WG
Energy based [87]	high	moderate	moderate	symmetric planar PTL
Even-odd mode [133, 134]	high	moderate	moderate	symmetric planar PTL
CRLH [8]	variable (1/f)	low	high	arbitrary planar PTL
Modified CRLH [VI, VII]	high	low	low	arbitrary planar PTL

5. Experimental validation

The aim of experimental validation within the frame of this work was to verify the through broad-side scanning capability of a MEMS based leaky-wave antenna to confirm the design procedure of periodic TLs, and to observe the radiation pattern of leaky-wave antennas based on this periodic TL. This work was partially sponsored by the Tekes and European Framework Program 7 in order to develop new standards for future automotive radar technology within the SARFA (Steerable Antennas for Automotive Radar and Future Wireless Applications) and TUMESA (Tuneable Metamaterials for Smart Wireless Applications) projects respectively. The MEMS device was the crucial implementation technology to be used due to its potentially superior performance compared to other steering techniques discussed.

5.1 MEMS based implementation

Given the high demands of emerging automotive radar standards, such as the large scale of integration and high operating frequencies (77 GHz), clean room fabrication processes are required in order to fully utilize the advantages afforded by MEMS technologies. Based on cooperation with KTH, Sweden, a MEMS based leaky-wave antenna was fabricated. The fabrication consists of a number of steps and is jointly called 'process flow', which differs from structure to structure and is essentially a sequence of technological processes needed to fabricate a given structure. More about microfabrication processes and process flow in general can be found in [143]. For our purposes the process flow included the following procedures: adhesive wafer bonding; patterning of the MEMS electrodes on the silicon substrate; stripping of support wafers; metallization of silicone membrane; patterning; deep reactive iron etching (DRIE); and finally, wire-bonding to provide connection of the MEMS to the ground plane. The fabrication process is described in more detail in [IV].

Since every microfabrication process flow is subject to research and optimization [143], no universal procedure can be prescribed. Especially in the case of leaky-wave antennas, the microfabrication process is challenging and would in itself be enough for another dissertation.

Within the framework of SARFA and TUMESA projects, samples of leaky-wave antennas based on microstrip line loaded with MEMS capacitors were fabricated (at KTH, Sweden) and measured (at VTT, Finland).

A leaky-wave antenna based on a microstrip line loaded with MEMS has been analytically and numerically studied in [II]. The scanning capability with changing MEMS capacitance with realistic tuning ratio of 2 was found to be in the range from θ = -22° to +21° (see Fig. 25).

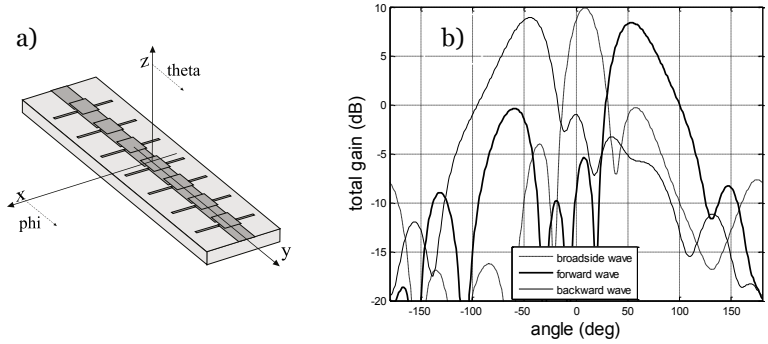

Figure 25a Sketch of studied leaky-wave antenna with coordinate system, **b** Plot of total gain of studied antenna (*yz* plane cut) –for the tuning ratio higher than 2 [III].

Out of the many samples fabricated, S-parameters of those with capacitance C_L such that the whole structure is out of balance were measured. The overlapping area of the MEMS membrane and the microstrip line determining the C_L capacitance was the variable. Changing the overlapping (see Fig. 26), the resonance frequencies of the structure change (increase in overlapping decreases the resonance frequency). In Fig. 27 the comparison of measured and simulated data is displayed and confirms the assumed behavior [IV].

Since the continuously tunable MEMS [144] for millimeter-waves applications remains to become fully matured technology, the experimental validation of a fixed frequency beam scanning leaky-wave antenna (LWA) at 77 GHz was omitted. The concept of a fixed frequency scanning LWA was validated using a lower frequency (26 GHz) design based on a microstrip TL loaded with an interdigital capacitor and short microstrip section stub inductor. The results of this study are discussed in the following section.

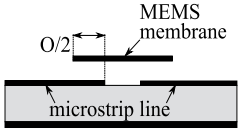

Figure 26 Overlapping *O* (determining the MEMS series capacitance) of the MEMS membrane and microstrip line (side view).

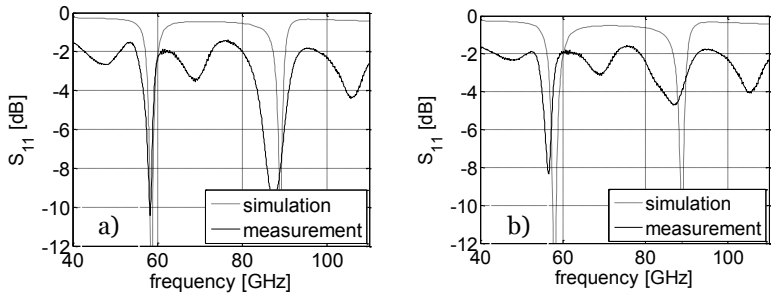

Figure 27 Comparison of simulated and measured results for different overlapping of the MEMS membrane and microstrip line **(a)** 10 μm, **(b)** 20 μm [IV].

5.2 Microstrip implementation at 26 GHz

The implementation of a leaky-wave antenna at 26 GHz enabled confirmation of the design method for finite transmission lines based on planar lines, and permitted verification of the concept of fixed frequency scanning, via the change of one of the constitutive parameters of the loaded TL, which in this case, was the capacitance of the interdigital capacitor.

Several substrates were considered for the fabrication and eventually RT Duroid 5880 with relative permittivity ε_r = 2.2, loss tangent tanδ = 0.0009 and thickness h = 787 μm and metallization thickness t = 35 μm was chosen. A microstrip line with an impedance of 50 Ω was designed to comply with the measurement equipment.

In order to verify the design method described in Chapter 4.3, a number of cascades centered around 26 GHz were designed. Applying the design method we obtained the dimensions of the capacitor finger length, l_{CAP}, and the length of the inductor, l_{IND}, shown in Fig. 28.

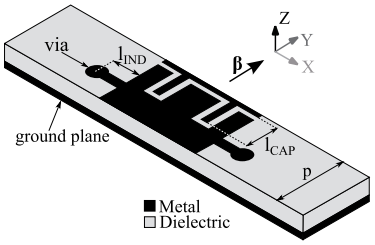

Figure 28 Drawing of a unit cell of the verification structure, with period length, p, capacitor finger overlapping, l_{CAP}, and inductor length, l_{IND} [VI].

The dimensions are shown in the Table II and are different for each cascade with N cells as expected. Simulation results for this structure are shown in Fig. 29 and 30 where the magnitude of scattering parameter S_{11} and the dispersion curves are shown, respectively.

Table II Dimensions of fabricated structures with increasing cell numbers, *N*, and corresponding dimensions of the elements, shown in Fig. 27

N [-]	l_{IND} [mm]	l_{CAP} [mm]
1	0.52	0.68
2	0.49	0.70
3	0.48	0.71
4	0.46	0.72
5	0.45	0.72
6	0.44	0.73
10	0.42	0.74

Cascades are visibly balanced around the design frequency, resulting in very good matching at 26 GHz, and the dispersion curves have almost zero band-gap corresponding to the balanced state.

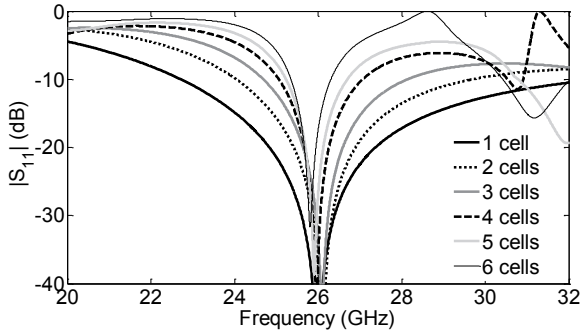

Figure 29 Simulation results of scattering parameters for structures with varying number of cascaded cells centered at 26 GHz.

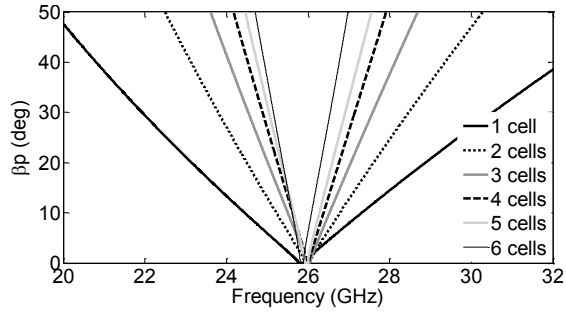

Figure 30 Simulation results of dispersion curves for structures with varying number of cascaded cells centered at 26 GHz.

In Fig. 31, the resulting measurement of the scattering parameters for a structure composed of 20 cells is shown. Overall good agreement can be observed, and especially around the main resonance frequency with very good matching. In order to verify the balance of the structure, the radiation patterns were measured in *YZ* plane, according to Fig. 25a. If the designed structures are balanced, we should observe a through broad side frequency scanning capability. The periodic TLs designed can thus be described in terms of periodic leaky-wave antennas.

Simulation results of frequency scanning in the range of 23 – 29 GHz are displayed in Fig. 32.

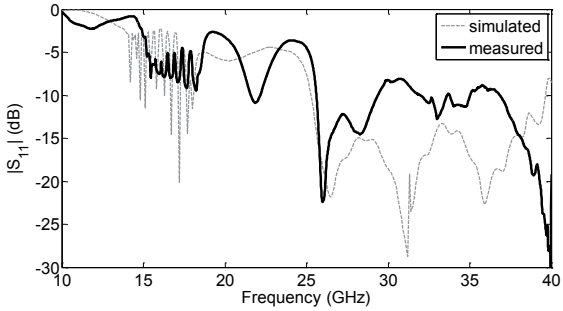

Figure 31 Comparison of measured and simulated results for a 20 cell structure [VI].

The range of the scanning angles for this frequency band is observed to be from -13° to 30°. In order to measure fabricated samples, 3.5 mm coaxial connectors were soldered to the structures. Ample agreement can be observed from the comparison of measured and simulated radiation patterns and maximum gain, see Fig. 33 and 34 respectively. Slight deterioration occurs for backward wave operation (23-25 GHz) due to the vicinity of the transition coaxial-microstrip [VI], which disturbs the radiated fields. For example, a side lobe at approximately 60° can be observed with most of the patterns due to the radiation caused by the transition [VI]. Full 3D measurement was not possible with regard to time and equipment constraints. The maximum directivity (and efficiency) of the twenty cell structure was estimated based on the measurements of radiation patterns of co-polar components in principal planes. This approximation is limited for antennas with one major lobe with low sidelobes. However, the sidelobes present in our structure decreased the accuracy of the approximation to such degree that we opted to exclude these results from final manuscript. Simulated radiation efficiency does not drop below 92 % in the whole band 23-29 GHz.

The main purpose of this experiment was to verify the functionality of the design procedure, i.e., the ability of the periodic transmission line (PTL) to scan the main beam angle through broad side with sweeping frequency, which was confirmed.

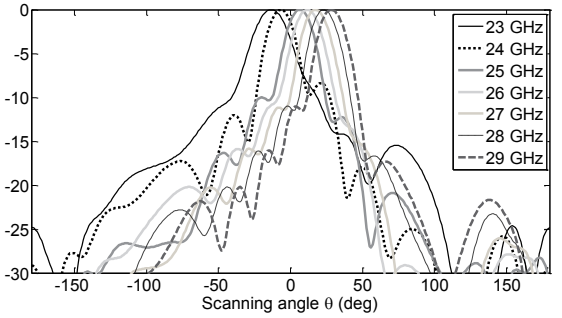

Figure 32 Simulated results of radiation patterns for 20 cell structure [VI].

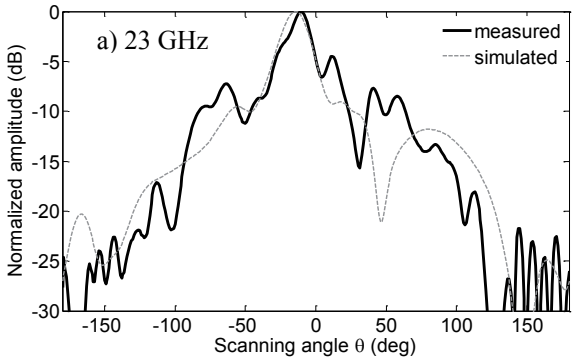
a) 23 GHz
measured
simulated
Normalized amplitude (dB)
0
-5
-10
-15
-20
-25
-30
-150
-100
-50
0
50
100
150
Scanning angle θ (deg)

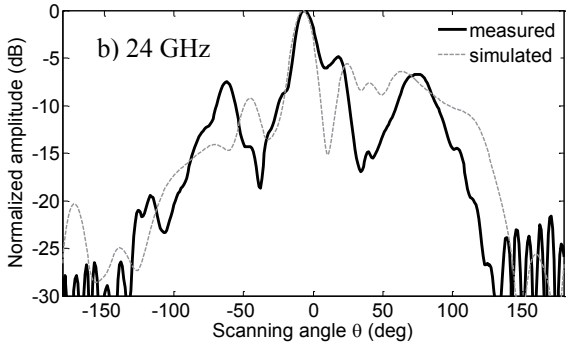
b) 24 GHz
measured
simulated
Normalized amplitude (dB)
0
-5
-10
-15
-20
-25
-30
-150
-100
-50
0
50
100
150
Scanning angle θ (deg)

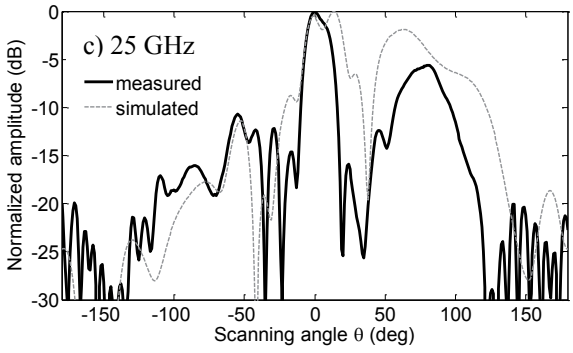
c) 25 GHz
measured
simulated
Normalized amplitude (dB)
0
-5
-10
-15
-20
-25
-30
-150
-100
-50
0
50
100
150
Scanning angle θ (deg)

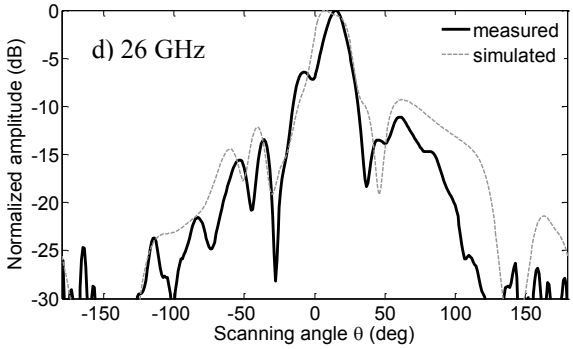
d) 26 GHz
measured
simulated
Normalized amplitude (dB)
0
-5
-10
-15
-20
-25
-30
-150
-100
-50
0
50
100
150
Scanning angle θ (deg)

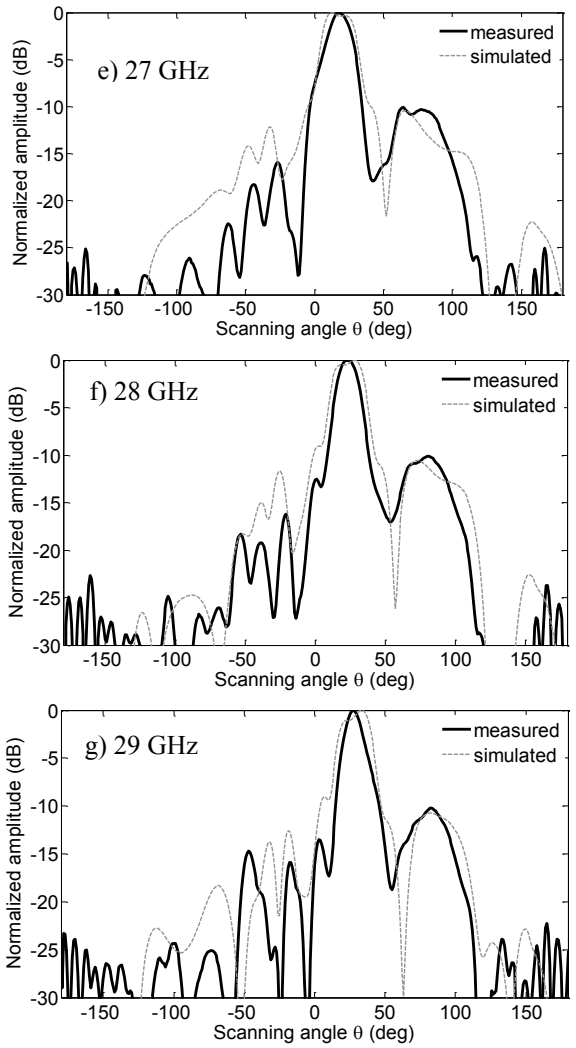

Figure 33a)-g) Comparison of measurement and simulation results of radiation patterns of a 20 cell structure for given frequencies [VI].

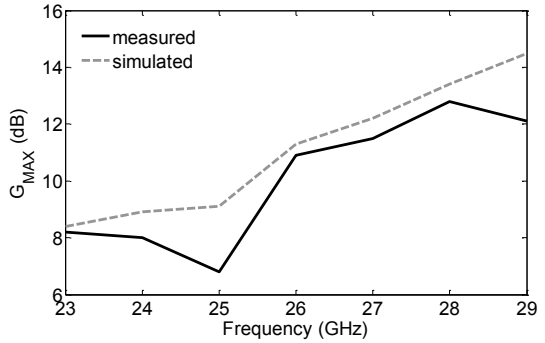

Figure 34 Comparison of measured and simulated maximum gain of a 20 cell structure.

Experimental verification includes also a fixed frequency scanning thirty cell structure at 26 GHz. Immaturities of MEMS technology, in terms of continuous capacitance change, resulted in the choice of an alternative structure with an interdigital capacitor.

Measurements of the samples with different capacitance values at a single frequency point confirmed the concept of fixed frequency scanning see Fig. 35. Since the aim of this experiment was to verify the scanning capabilities of the antenna, a thirty cell structure was manufactured based on the twenty cell structure, i.e. with the same dimensions. Fine tuning of the structure was omitted, and therefore the broadside performance of the antenna is not optimal. The observed scanning range is ±15 degrees (capacitance range from 40 to 110 fF, yielding a tuning ratio of 2.9), which is sufficient angular range for long range automotive radar [145], or adaptive of communication links [146]. The future success of MEMS as a quasi-continuous tuning element for millimeter-wave devices is dependent on the technological readiness in terms of achievable tuning range (up-to-date MEMS typically have maximum tuning ratio from 2 to 2.5) and reconfigurability.

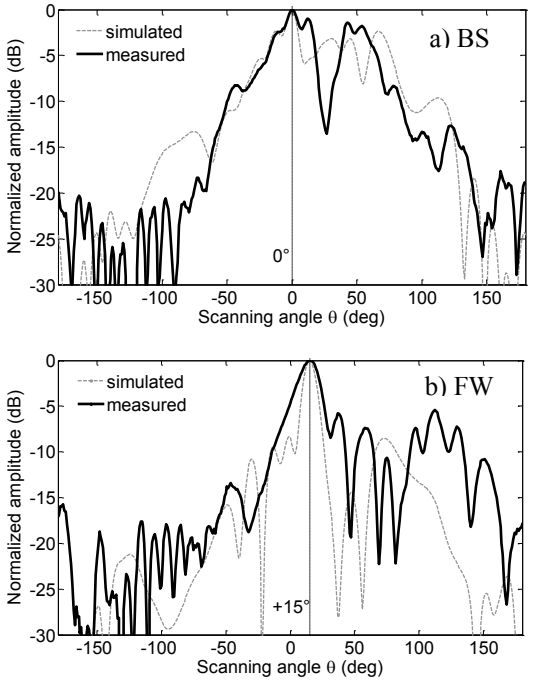

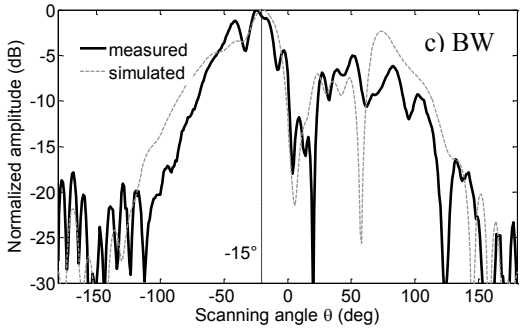

Figure 35 Comparison of measured and simulated radiation patterns of a 30 cell structure at fixed frequency 26 GHz, a) broadside wave, b) forward wave with main beam angle 15 degrees, and c) backward wave with radiation angle -15 degrees.

6. Summary of publications

Publication [I]: "Leaky-wave regimes on MEMS-loaded transmission lines for mm-wave applications**"**

Microstrip line, coplanar waveguide, capacitively shorted coplanar waveguide, and coplanar stripline are analyzed in terms of metamaterial transmission lines, more precisely in terms of the Bloch analysis. The main focus is on dispersive properties and in particular the possibility of achieving fast-wave propagation. MEMS capacitors are used in combination of shunt inductors to achieve this to be utilized for a leaky-wave antenna with significantly reduced losses compared to conventionally used diode varactors or magnetized ferrites. The dispersion and Bloch impedance are the observed parameters to determine the fast-wave propagation. Eventually the coplanar stripline and microstrip based leaky-wave antennas are numerically analyzed confirming the leaky-wave radiation.

Publication [II]: "Beam-steering MEMS-loaded antenna based on planar transmission lines"

Periodically loaded coplanar waveguide (periodic transmission line – PTL) is studied in this paper. Analytical and numerical analysis of suggested model is performed to investigate the dispersive properties of the planar transmission line loaded with a series capacitor, in this case a microelectromechanical (MEMS) capacitor, and a shunt inductor, in this case a short section of a microstrip. Initially a single unit cell of the PTL is studied and characterized. Radiation properties of the PTL are studied with structure composed of a cascade of the cell studied beforehand. It is verified that changing the MEMS capacitance, the angle of main beam radiation can be effectively steered.

Publication [III]: "Leaky-wave antenna based on microelectromechanical systems-loaded microstrip line**"**

An analytical model of a PTL is used to design a unit cell of a leaky-wave antenna loaded with MEMS capacitors and shunt inductors. Analysis and design are done through particle swarm optimization implemented in

Matlab and in numerical full-wave simulation software. Main beam radiation of the designed leaky-wave antenna is scanned from backward to forward direction with a seamless transition through broadside through changing capacitance of MEMS by increasing and decreasing the gap of the membrane above the transmission line. With a realistic capacitance ratio of 2 a scanning range is achieved to comply with future automotive far-sight anti-collision radar.

Publication [IV]: "Leaky-wave antenna at 77 GHz**"**

Previously designed leaky-wave antenna based on microstrip line loaded with MEMS capacitors and shunt inductors was modified to comply with the microfabrication constraints. Bonding wires and bonding pads connecting the inductors were added in order to connect the inductors to the ground plane. Fabrication of the samples consisted of ten processes described in detail in the paper. Measurements results of two samples showed good agreement with simulation.

Publication [V]: "W-band substrate integrated waveguide technology for scanning antenna architectures**"**

Scanning antenna architecture operating in the W-band was designed based on the leaky-wave antenna concept. The system consists of a number of substrate integrated waveguide based antennas depending on how wide angular scanning range is supposed to be covered. In our case the antenna system covers wide angular range starting from 7 to 56 degrees which is achieved by frequency scanning from 88 to 94 GHz. Return losses of the antennas are better than 10 dB in the whole band of interest and the beam width is 10°±3°.

Publication [VI]: "A systematic design method for CRLH periodic structures in the microwave to millimeter-wave range**"**

A precise methodology for design of periodic transmission lines based on planar lines is introduced in this paper. Inter-cell and intra-cell coupling are the main factors influencing the structure. Underlying physics of these effects are described and compensated. The relevance of the method proposed is increasing with increasing frequency, where the parasitic capacitive susceptances and inductive reactances have increasing influence. A microstrip based structure is designed and simulated at 77 and 26 GHz. The 26 GHz structure is fabricated and measured to verify the functionality of the method. Besides scattering parameters, radiation patterns are

measured as well to verify the through-broadside scanning capability of the balanced metamaterial transmission line.

Publication [VII]: "Design aspects of finite periodic transmission lines based on planar structures**"**

Detailed analysis of the relations within the unit cell of a periodic transmission line based on planar lines is done in this paper. Structures with electrical size of the unit cell in the range from 0.1 to $0.54\lambda_G$ are studied and evaluated in terms of the overall performance of the final structure and ease of design. General design guidelines are described with regard on the most influential parameters – electrical size, fabrication inaccuracies, and center frequency of operation.

7. Conclusions and future research

In this thesis the periodic transmission lines have been investigated. At the beginning of the research, the main goal was to design a leaky-wave antenna for millimeter wavelengths based on planar transmission lines with electrically reconfigurable scanning capability. On the way to this end, many unanswered questions have arisen.

The initial task was to investigate the dispersive properties of planar lines and to choose suitable option for experimental verification. Based on the analysis made, a general remark can be made, i.e. that the majority of the lines are capable to support desired dispersive behavior, though the ones with a ground plane are more suitable for the leaky-wave antenna for scanning radar application owing to the fact that the power is radiated mainly into one half space, improving the directive properties of the structure.

Although leaky-wave antennas have been investigated extensively over the last decades, the transmission line based leaky-wave antennas have received considerable attention mainly since the advent of metamaterials. The state of the art of design of metamaterial leaky-wave antennas based on planar transmission lines mainly employs circular approach, i.e. initial design, subsequent analysis and correction of the structure until desired properties are reached. In this work a linear approach was introduced, i.e. design of the PTL structure with no recurrent loops.

Since the original purpose was to design an electrically reconfigurable leaky-wave antenna for future automotive radar standards operating at 77 GHz, the desired antenna pattern is thus ideally a fan beam shaped lobe with zero back radiation and zero sidelobes. Therefore a microstrip implementation was chosen to keep the back radiation at minimum. The microstrip-based leaky-wave antenna design was numerically analyzed and validated with a MEMS varactor as a tuning element with scanning performance confirming the long range radar requirements.

An inherent inconsistency and imprecision of the design methods based on numerical approach was revealed during the design of periodic leaky-wave antennas, particularly when increasing the operation frequencies into the millimeter-wave range. Hence, an efficient and easy to use method based on

the compensation of parasitic elements and periodicity was developed for the design of PTLs based on planar lines covering the frequency range from a DC to approximately 100 GHz. Additional advantage of this method is that it can be generalized for a group of planar TL loaded with distributed elements with minor modifications, depending on the specific topology of the loading elements.

Based on this method, a periodic leaky-wave antenna was designed and experimentally verified at 26 GHz. The through-broadside frequency scanning capability was observed, confirming the functionality of the method. Exchanging the MEMS varactor for an interdigital capacitor structure, due to the lack of technological readiness, we verified the possibility of scanning the main beam in the range of angles needed in order to be utilized for emerging automotive radar standards. The future usage of MEMS varactors depends on the maturity of the technology, particularly with regard to the long term performance and stability.

The upper frequency limit of 100 GHz for the design method is only approximate. It was not tested beyond 77 GHz, thus the future research lies in extending the frequency span of its applicability. Additional extension of usage can be made with regard to different metamaterial structures. Since the metamaterial transmission line serves as a basis for many other applications besides antennas, there is a potential to develop efficient ways of design for two and possibly even 3-D metamaterial structures.

PTLs represent a versatile platform for implementing metamaterial structures. For many applications the planar technology is especially suitable due to its high level of maturity and affordable price. Nevertheless, lasting challenges and dependency on technological readiness drive the research of metamaterial transmission lines further ahead.

References

[1] W. Rotman, "Plasma simulation by artificial dielectrics and parallel plate media," *IRE Trans. Antennas Propag.,* no. 10, pp. 82–95, 1962.

[2] G. H. B. Thompson, "Backward waves in longitudinally magnetized ferrite filled guides," *Proc. of Symp. on Electromagnetic Theory and Antennas*, Copenhagen Denmark, vol. 6, June 1962, p. 591.

[3] V. G. Veselago, "The electrodynamics of substances with simultaneously negative values of ε and μ," *Soviet Phys. Usp.*, no. 10, pp. 509–514, 1968.

[4] D. R. Smith, W. J. Padilla, D. C. Vier, S. C. Nemat-Nasser, and S. Schultz, "Composite medium with simultaneously negative permeability and permittivity," *Phys. Rev. Lett.*, vol. 84, no. 18, pp. 4184-4187, 2000.

[5] S. A. Schelkunoff and H. T. Friis, *Antennas: Theory and practice,* New York NY, John Wiley & Sons, 1952.

[6] J. B. Pendry, "Negative refraction makes a perfect lens," *Phys. Rev. Lett.*, no. 85, pp. 3966–3969, 2000.

[7] R. A. Shelby, D. R. Smith, and S. Schultz, "Experimental verification of a negative index of refraction," *Science*, no. 292, pp. 77–79, 2001.

[8] C. Caloz and T. Itoh, *Electromagnetic Metamaterials Transmission Line Theory and Microwave Applications*, Hoboken NJ: John Wiley & Sons, Inc. Publication, 2006.

[9] S. Tretyakov, *Analytical Modeling in Applied Electromagnetics*, Norwood MA, Artech House, 2003.

[10] N. Engheta and R. W. Ziolkowski, Eds., *Electromagnetic Metamaterials: Physics and Engineering Explorations*, Piscataway NJ, Wiley-IEEE Press, 2006.

[11] T. J. Cui, D. R. Smith, and R. Liu, *Metamaterials: Theory, Design, and Applications*, NY, Springer, 2010.

[12] A. A. Oliner, "Leaky-wave antennas," in *Antenna Engineering Handbook*, Third Edition, edited by R. C. Johnson, New York NY, McGraw Hill, 1993.

[13] A. A. Oliner, "A periodic-structure negative-refractive-index medium without resonant elements," *IEEE-AP-S Digest*, San Antonio, Texas, 2002, p. 41.

[14] G. V. Eleftheriades and K. G. Balmain, Eds., *Negative-Refraction Metamaterials: Fundamental Principles and Applications*, Hoboken NJ, John Wiley & Sons, 2005.

[15] T. J. Cui, H. F. Ma, R. Liu, B. Zhao, Q. Cheng, and J. Y. Chin, "A symmetrical circuit model describing all kinds of circuit metamaterials," *Progr. Electromagn. Res. B*, no. 5, pp. 63–76, 2008.

[16] C. Caloz and T. Itoh, "Transmission-line approach of left-handed (LH) materials and microstrip implementation of an artificial LH transmission line," *IEEE Trans. Antennas Propag.*, vol. 52, no. 5, pp. 1159-1166, 2004.

[17] G. V. Eleftheriades, A. K. Iyer, and P. C. Kremer, "Planar negative refractive index media using periodically L-C loaded transmission lines," *IEEE Trans. Microw. Theory Techn.*, vol.50, no.12, pp. 2702- 2712, Dec. 2002.

[18] C. Simovski, "Bloch material parameters of magneto-dielectric metamaterials and the concept of Bloch lattices," *Metamaterials*, vol. 1, no. 2, pp. 62-80, 2007.

[19] A. Sihvola, *Electromagnetic Mixing Formulas and Applications*, London, UK, The Institution of Electrical Engineers, 1999.

[20] H. Ming-Kuei and D. Cheng, "A new class of artificial dielectrics," *Proceedings of WESCON Conference*, Aug. 1958, vol. 2, pp. 21-25.

[21] M. Bingle, J. H. Cloete, and D. B. Davidson, "Microwave absorption by chiral, racemic and non-chiral unit cells: the role of chirality in absorbing materials," *Proceedings of the South African Symposium on Communications and Signal Processing*, Rondebosch, South Africa, Sep. 1998, pp. 441-444.

[22] A. Sihvola, "Metamaterials in electromagnetics," *Metamaterials*, vol. 1, no. 1, pp. 2-11, March 2007.

[23] M. Lapine and S. Tretyakov, "Contemporary notes on metamaterials," *IET Proc.: Microwaves Antennas Propag.*, no. 1, vol. 1, pp. 3-11, 2007.

[24] A. Sihvola, "Electromagnetic emergence in metamaterials," in: S. Zhoudi, A. Sihvola, and M. Arsalane, *Advances in Electromagnetics of Complex Media and Metamaterials*, vol. 89, Kluwer Academic Publishers, Dordrecht, 2003, pp. 1-17 (NATO Science Series II: Mathematics, Physics, and Chemistry).

[25] W. E. Kock, "Metal lens antennas," *Proceedings of IRE*, vol. 34, pp. 828-836, Nov. 1946.

[26] M. Bayindir, K. Aydin, E. Ozbay, P. Markos, and C. M. Soukoulis, "Transmission properties of composite metamaterials in free space," *Appl. Phys. Lett.*, no. 81, pp. 120–122, 2002.

[27] R. B. Greegor, C. G. Parazzoli, K. Li, and M. H. Tanielian, "Origin of dissipative losses in negative index of refraction materials," *Appl. Phys. Lett.* vol. 82, no. 14, pp. 2356–2358, Apr. 2003.

[28] G. Dolling, M. Wegener, C. M. Soukoulis, and S. Linden, "Negative-index metamaterial at 780 nm wavelength," *Opt. Lett.*, vol. 32, no. 1, pp. 53-55, Jan. 2007.

[29] C. García-Meca, J. Hurtado, J. Martí, and A. Martínez, "Low-loss multilayered metamaterial exhibiting a negative index of refraction at visible wavelengths," *Phys. Rev. Lett.*, vol. 106, no. 6, Feb. 2011.

[30] S. A. Zhang, W. Fan, N. C. Panoiu, K. J. Malloy, R. M. Osgood, and S. R. J. Brueck, "Optical negative-index bulk metamaterials consisting of 2D perforated metal-dielectric stacks," *Opt. Express*, vol.14, no. 15, pp. 6778–6787, July 2006.

[31] A. Ahmadi and H. Mosallaei, "Physical configuration and performance modeling of all-dielectric metamaterials," *Phys. Rev. B*, no. 77, pp. 045104-1 – 9, 2008.

[32] J. A. Schuller, R. Zia, T. Taubner, and M. L. Brongersma, "Dielectric metamaterials based on electric and magnetic resonances of silicon carbide particles," *Phys. Rev. Lett.,* no. 99, pp. 104701-1 – 4, 2007.

[33] X. Cai, R. Zhu, and G. Hu, "Experimental study of metamaterials based on dielectric resonators and wire frame," *Metamaterials*, vol. 2, pp. 220–226, 2008.

[34] C. L. Holloway, E. F. Kuester, J. Baker-Jarvis, and P. Kabos, "A double negative (DNG) composite medium composed of magnetodielectric

spherical particles embedded in a matrix," *IEEE Trans. Antennas Propag.,* vol. 51, pp. 2596–2603, 2003.

[35] M. Decker, R. Zhao, C. M. Soukoulis, S. Linden, and M. Wegener, "Twisted split-ring-resonator photonic metamaterial with huge optical activity," *Opt. Lett.*, no. 35, pp. 1593–1595, 2010.

[36] D. O. Guney, T. Koschny, and C. M. Soukoulis, "Intra-connected three-dimensionally isotropic bulk negative index photonic metamaterial," *Opt. Express* 18, pp. 12348–12353, 2010.

[37] D. B. Burckel, J. R. Wendt, I. Brener, and M. B. Sinclair, "Dynamic membrane projection lithography," *Opt. Mat. Exp.*, vol. 1, no. 5, pp. 962–969, 2011.

[38] A. J. Hoffman, L. Alekseyev, S. S. Howard, K. J. Franz, D. Wasserman, V. A. Podolskiy, E. E. Narimanov, D. L. Sivco, and C. Gmachl, "Negative refraction in semiconductor metamaterials," *Nature Mater.*, no. 6, pp. 946–950, 2007.

[39] D. M. Pozar, *Microwave Engineering*, Hoboken NJ, John Wiley & Sons, Inc., 1998.

[40] P. Alitalo, O. Luukkonen, and S. Tretyakov, "A three-dimensional backward-wave network matched with free space," *Physics Letters A,* no. 372, pp. 2720–2723, 2008.

[41] Y. Wang, Y. Zhang, F. Liu, L. He, H. Li, H. Chen, and C. Caloz, "Simplified description of asymmetric right-handed composite right/left-handed coupler in microstrip chip technology," *Microwave Opt. Technol. Lett.*, vol. 49, no. 9, pp. 2063-2068, Sep. 2007.

[42] C. Caloz, A. Sanada, and T. Itoh, "A novel composite right/left-handed coupled-line directional coupler with arbitrary coupling level and broad bandwidth," *IEEE Trans. Microw. Theory Techn.*, vol. 52, no. 3, pp. 980-992, March 2004.

[43] P. P. Wang, M. A. Antoniades, and G. V. Eleftheriades, "An investigation of printed Franklin antennas at X-band using artificial (metamaterial) phase shifting lines," *IEEE Trans. Antennas Propagat.*, vol. 56, no. 10, pp. 3118-3128,

[44] D. Kholodnyak, E. Serebryakova, I. Vendik, and O. Vendik, "Broadband digital phase shifter based on switchable right- and left-handed transmission line sections," *IEEE Microw. Wireless Compon. Lett.*, vol. 16, no. 15, pp. 258-260, May 2006.

[45] M. A. Antoniades and G. V. Eleftheriades, "A broadband series power divider using zero-degree metamaterial phase-shifting lines," *IEEE Microw. Wireless Compon. Lett.*, vol. 15, no. 11, pp. 808-810, Nov. 2005.

[46] H. V. Nguyen and C. Caloz, "Tunable arbitrary N-port CRLH infinite wavelength series power divider," *Electronics Lett.*, vol. 43, no. 23, Nov. 2007.

[47] J.-H. Park, Y.-H. Ryu, J.-G. Lee, and J.-H. Lee, "Epsilon negative zeroth-order resonator antenna," *IEEE Trans. Antennas Propagat.*, vol. 55, no. 12, pp. 3710-3712, Dec. 2007.

[48] B. Pillans, S. Eshelman, A. Malczewski, J. Ehmke, and C. Goldsmith, "Ka-band RF MEMS phase shifters," *IEEE Microw. Guided Wave Lett.*, vol. 9, no. 12, pp. 520-522, Dec. 1999.

[49] S. Y. Kim and G. M. Rebeiz, "A 4-bit passive phase shifter for automotive radar applications in 0.13 μm CMOS," IEEE Compound Semiconductor Integrated Circuit Symposium, Greensboro, NC, USA, Oct. 2009.

[50] K. Maruhashi, H. Mizutani, and K. Ohata, "A Ka-band 4-bit monolithic phase shifter using unresonated FET switches," *IEEE MTT-S International Microwave Symposium Digest*, June 1998, pp. 51-54.

[51] H. Wu and Y. Chan, "Tunable high-Q MMIC active filter by negative resistance compensation," *Gallium Arsenide Integrated Circuit Symposium*, Anaheim CA, Oct. 1997, pp. 252-255.

[52] P-Y. Chen, T-W. Huang, H. Wang, Y-C. Wang, C-H. Chen, and P-C. Chao, "K-band HBT and HEMT monolithic active phase shifters using vector sum method," *IEEE Trans. Microw. Theory Tech.*, vol. 52, no. 5, pp. 1414-1424, May 2004.

[53] C. Weil, S. Müller, P. Scheele, Y. Kryvoshapka, G. Lüssem, P. Best, and R. Jakoby, "Ferroelectric- and liquid-crystal tunable microwave phase shifters," *Proceedings of 33rd European Microwave Conference*, Munich, Germany, Oct. 2003, pp. 1431-1434.

[54] J. G. Yang and K. Yang, "Ka-Band 5-bit MMIC phase shifter using InGaAs PIN switching diodes," *IEEE Microw. Wireless Compon. Lett.*, vol. 21, no. 3, pp. 151-153, March 2011.

[55] C. Vittoria, "Ferrite uses at millimeter wavelengths," *Journal of Magnetic Materials*, vol. 21, no. 2, pp. 109-118, 1980.

[56] S. Sirci, J. D. Martinez, M. Taroncher, and V. E. Boria, "Analog tuning of compact varactor-loaded combline filters in substrate integrated waveguide," *Proceedings of 42nd European Microwave Conference*, Amsterdam, Netherlands, Oct.–Nov. 2012, pp. 257-260.

[57] Ch. Rauscher, "Reconfigurable bandpass filter with three-to-one switchable passband width," *IEEE Trans. Microw. Theory Techn.,* vol. 51, no. 2, pp. 573-577, Feb. 2003.

[58] C. Lugo, G. Wang, J. Papapolymerou, Z. Zhao, X. Wang, and A. T. Hunt, "Frequency and bandwidth agile millimeter-wave filter using ferroelectric capacitors and MEMS cantilevers," *IEEE Trans. Microw. Theory Techn.*, vol. 55, no. 2, pp. 376 – 382, Feb. 2007.

[59] Y. Murakami, T. Ohgihara, and T. Okamoto, "A 0.5-4.0 GHz tunable bandpass filter using YIG film grown by LPE," *IEEE Trans. Microw. Theory Techn.*, vol. 35, no. 12, pp. 1192 – 1198, Dec. 1987.

[60] I. Bahl and P. Bhartia, *Microwave Solid State Circuit Design*, Hoboken NJ, Wiley Interscience, May 2003.

[61] Z. Zhao, X. Wang, K. Choi, C. Lugo, and A. T. Hunt, "Ferroelectric phase shifters at 20 and 30 GHz," *IEEE Trans. Microw. Theory Tech.*, vol. 55, no. 2, pp. 261-264, Feb. 2004.

[62] G. Rebeiz, *RF MEMS Theory, Design and Technology*, Hoboken NJ, John Wiley & Sons, Feb. 2004.

[63] V. Vardan, K. J. Vinoy, and K. A. Jose, *RF MEMS and Their Applications*, Chichester, UK, John Wiley & Sons Ltd, 2003.

[64] I. Reines, S.-J. Park, and G. M. Rebeiz, "Compact Low-Loss Tunable X-band bandstop filter with miniature RF-MEMS switches," *IEEE Trans. Microw. Theory Tech.*, vol. 58, no. 7, pp. 1887-1895, July 2010.

[65] D. Chicherin, S. Dudorov, D. Lioubtchenko, V. Ovchinnikov, and A. V. Räisänen, "Millimetre wave phase shifters based on a metal waveguide

with a MEMS-based high impedance surface," *Proceedings of the 36th European Microwave Conference*, Manchester, UK, Sep. 2006, pp. 372-375.

[66] Y. Lu, L. P. B. Katehi, and D. Peroulis, "High-power MEMS varactors and impedance tuners for millimeter-wave applications," *IEEE Trans. Microw. Theory Tech.*, vol. 53, no. 11, pp. 3672-3678, Nov. 2005.

[67] I. E. Pehlivanoglu, C. A. Zorman, and D. J. Young, "Silicon carbide MEMS oscilator," *Proceedings of International Conference on Solid-State Sensors, Actuators and Microsystems*, Denver, CO, USA, June 2009, pp. 569-572.

[68] J.-P. Raskin, A. R. Brown, B. T. Khuri-Yakub, and G. M. Rebeiz, "A novel parametric-effect MEMS amplifier," *J. Microelectromech. Syst.*, vol. 9, no. 4, pp. 528-537, Dec. 2000.

[69] J. Hong and M. J. Lancaster, *Microstrip Filters for RF/Mircorwave Applications*, New York, NY, John Wiley & Sons, Apr. 2004.

[70] J. Robinson and Y. Rahmat-Samii, "Particle swarm optimization in electromagnetics," *IEEE Trans. Antennas Propag.*, vol. 52, no. 2, pp. 397-407, 2004.

[71] J. Perruisseau-Carrier, T. Lisec, and A. K. Skrivervik, "Circuit model and design of silicon-integrated CRLH-TLs analogically controlled by MEMS," *Microw. Opt. Technol. Lett.*, vol. 48, no. 12, pp. 2496-2499, Dec. 2006.

[72] M. A. Llamas, D. Girbau, E. Pausas, L. Pradell, S. Aouba, C. Villeneuve, V. Puyal, P. Pons, R. Plana, S. Colpo, and F. Giacomozzi, "Capacitive and resistive RF-MEMS switches 2.5D & 3D electromagnetic and circuit modeling," *Proceedings of Spanish Conference on Electron Devices*, Santiago de Compostela, Spain, Feb. 2009, pp. 451-454.

[73] J. Iannacci, R. Gaddi, and A. Gnudi, "Non-linear electromechanical RF model of a MEMS varactor based on VerilogA© and lumped-element parasitic network," *Proceedings of the 2nd European Microwave Integrated Circuits Conference*, Munich, Germany, Oct. 2007, pp. 544-547.

[74] T. Kim, Z. Marinković, V. Marković, M. Milijić, O. Pronić-Rančić, and L. Vietzorreck, "Efficient modeling of an RF MEMS capacitive shunt switch with artificial neural networks," *Proceedings of URSI International Symposium on Electromagnetic Theory (EMTS)*, Hiroshima, Japan, May 2013, pp. 550-553.

[75] E. Erdil, K Topalli, M. Unlu, O. A. Civi, and T. Akin, "Frequency tunable microstrip patch antenna using RF MEMS technology," *IEEE Trans. Antennas Propagat.*, vol. 55, no. 4, pp. 1193-1196, Apr. 2007.

[76] C. W. Jung, M. J. Lee, G. P. Li, F. De Flaviis, "Reconfigurable scan-beam single-arm spiral antenna integrated with RF-MEMS switches," *IEEE Trans. Antennas Propagat.*, vol. 54, no. 2, pp. 455-463, Feb. 2006.

[77] L. Petit, L. Dussopt, J. M. Laheurte, "MEMS-switched parasitic-antenna array for radiation pattern diversity," *IEEE Trans. Antennas Propagat.*, vol. 54, no. 9, pp. 2624-2631, Sep. 2006.

[78] J. Perruisseau-Carrier and A. K. Skrivervik, "Monolithic MEMS-based reflectarray cell digitally reconfigurable over a 360° phase range," *IEEE Antennas Wireless Propag. Lett.*, vol. 7, pp. 138-141, Feb. 2008.

[79] T. Kim, J. Kang, W. Che, and L. Vietzorreck, "Development of a tunable antenna using RF-MEMS based CRLH-transmission lines," *21st*

International Conference on Applied Electromagnetics and Communications (ICECom), Dubrovnik, Croatia, Oct. 2013.

[80] J. Sor, Ch. Chang, Y. Qian, and T. Itoh, "A reconfigurable leaky-wave/patch microstrip aperture for phased-array applications," *IEEE Trans. Microw. Theory Techn.*,vol. 50, no. 8, pp. 1877-1884, Aug. 2002.

[81] L. Huang, J.C. Chiao, and M.P. De Lisio, "An electronically switchable leaky wave antenna," *IEEE Trans. Antennas Propagat.*, vol. 48, no. 11, pp. 1769-1772, Nov. 2000.

[82] Y. Yashchyshyn, J. Marczewski, K. Derzakowski, J.W. Modelski, and P.B. Grabiec, "Development and investigation of an antenna system with reconfigurable aperture," *IEEE Trans. Antennas Propagat.*, vol. 57, no. 1, pp. 2-8, Jan. 2009.

[83] S. Lim, C. Caloz, and T. Itoh, "Electronically scanned composite right/left handed microstrip leaky-wave antenna," *IEEE Microw. Wireless Compon. Lett.*, vol. 14, no. 6, pp. 277-279, June 2004.

[84] G. Lovat, P. Burghignoli, and S. Celozzi, "A tunable ferroelectric antenna for fixed-frequency scanning applications," *IEEE Antennas Wireless Propag. Lett.*, vol. 5, pp. 353–356, Dec. 2006.

[85] V. K. Varadan, V. V. Varadan, K. A. Jose, and J. F. Kelly, "Electronically steerable leaky wave antenna using a tunable ferroelectric material," *Smart Mater. Struct.*, vol. 3, pp. 470–475, 1994.

[86] R. E. Collin, *Field Theory of Guided Waves, 2nd Edition*, New York, USA, IEEE Press, 1991.

[87] A. A. Oliner, "Radiating periodic structures: analysis in terms of k vs. β diagrams," *Short course on Microwave Field and Network Techniques*, Polytechnic Institute of Brooklyn, NY, USA, 4. June 1963.

[88] J. R. Pierce, "Coupling of modes of propagation," *J. Appl. Phys.*, vol. 25, pp. 179-183, 1954.

[89] P. Baccarelli, S. Paulotto, D. R. Jackson, and A. A. Oliner, "A new Brillouin dispersion diagram for 1-D periodic printed structures," *IEEE Trans. Antennas Propagat.*, vol. 55, no. 7, pp. 1484-1495, July 2007.

[90] L. Goldstone and A. Oliner, "Leaky-wave antennas I: Rectangular waveguides," *IRE Trans. Antennas Propag.*, vol. 7, no. 4, pp. 307-319, Oct. 1959.

[91] J. N. Hines and J. R. Upson, "A wide aperture tapered-depth scanning antenna," *Ohio State Univ. Res. Found.,* Report 667-7, Columbus, Ohio, Dec. 1957.

[92] W. W. Hansen, "Radiating electromagnetic waveguide," U.S. Patent No. 2, 402, 622, 1940.

[93] W. Rotman and N. Karas, "The sandwich wire antenna: A new type of microwave line source radiator," *IRE Conv. Rec.,* part 1, p. 166, 1957.

[94] D. R. Jackson and N. G. Alexopoulos, "Gain enhancement methods for printed circuit antennas," *IEEE Trans. Antennas Propag.*, vol. 33, no. 9, pp. 976-987, Sep. 1985.

[95] G. von Trentini, "Partially reflecting sheet arrays," *IEEE Trans. Antennas Propagat.*, vol. 4, no. 4, pp. 666-671, Oct. 1956.

[96] D. Sievenpiper, "High-impedance electromagnetic surfaces," Ph.D. thesis, University of California, Los Angeles, 1999.

[97] P. Baccarelli, P. Burghignoli, G. Lovat, and S. Paulotto, "Surface-wave suppression in a double-negative metamaterial grounded slab," *IEEE Antennas Wireless Propag. Lett.*, vol. 2, pp. 269-272, 2003.

[98] N. Engheta, "Thin absorbing screens using metamaterial surfaces," *IEEE Antennas and Propag. Soc. Int. Symposium*, vol.2, 2002, pp. 392-395.

[99] C. R. Simovski, P. A. Belov, and S. He. "Backward wave region and negative material parameters of a structure formed by lattices of wires and split-ring resonators," *IEEE Trans. Antennas Propagat.,* vol. 51, no. 10, pp. 2582–2591, Oct. 2003.

[100] J. Bonache, I. Gil, J. García-García, and F. Martín, "Novel microstrip bandpass filters based on complementary split-ring resonators," *IEEE Trans. Microw. Theory Tech.*, vol. 54, no. 1, pp. 265-271, 2006.

[101] J. Liu, D. R. Jackson, and Y. Long, "Substrate integrated waveguide (SIW) leaky-wave antenna with transverse slots," *IEEE Trans. Antennas Propag.*, vol. 60, no. 1, pp. 20-29, Jan. 2012.

[102] C. Jin, A. Alphones, and L. C. Ong, "Broadband leaky-wave antenna based on composite right/left handed substrate integrated waveguide," *IET Electronics Letters*, vol. 46, no. 24, pp. 1584-1585, Nov. 2010.

[103] M. Ettorre, R. Sauleau, and L. Le Coq, "Multi-beam multi-layer leaky-wave SIW pillbox antenna for millimeter-wave applications," *IEEE Trans. Antennas Propagat.*, vol. 59, no. 4, pp. 1093-1100, Apr. 2011.

[104] Z. Mekkioui and H. Baudrand, "Bi-dimensional bi-periodic center-fed microstrip leaky-wave antenna analysis by a source modal decomoposition in spectral domain," *IET Microw. Antennas Propag.*, vol. 3, no. 7, pp. 1141-1149, Oct. 2009.

[105] C. A. Balanis and C. R. Birtcher, *Leaky-wave antennas*, in *Modern Antenna Handbook*, Hoboken, NJ, USA, John Wiley & Sons, 2007.

[106] F. Xu and K. Wu, "Guided-wave and leakage characteristics of substrate integrated waveguide," *IEEE Trans. Microw. Theory Techn.*, vol. 53, no. 1, pp. 66-73, Jan. 2005.

[107] T. Tamir and A. A. Oliner, "Guided complex waves, Part I: Fields at an interface," *Proc. Inst. Elec. Eng.*, vol. 110, pp. 310-324, Feb. 1963.

[108] T. Tamir and A. A. Oliner, "Guided complex waves, Part II: Relation to radiation patterns," *Proc. Inst. Elec. Eng.*, vol. 110, pp. 325-334, Feb. 1963.

[109] Y. Cheng, W. Hong, K. Wu, and Y. Fan, "Millimeter-wave substrate integrated waveguide long slot leaky-wave antennas and two-dimensional multibeam applications," *IEEE Trans. Antennas Propagat.*, vol. 59, no. 1, pp. 40-47, Jan. 2011.

[110] F. Xu, K. Wu, and X. Zhang, "Periodic leaky-wave antenna for millimeter wave applications based on substrate integrated waveguide," *IEEE Trans. Antennas Propagat.*, vol. 58, no. 2, pp. 340-347, Feb. 2010.

[111] A. J. Martinez-Ros, J. L. Gomez-Tornero, and G. Goussetis, "Planar leaky-wave antenna with flexible control of the complex propagation constant," *IEEE Trans. Antennas Propagat.*, vol. 60, no. 3, pp. 1625-1630, March 2012.

[112] A. Martinez-Ros, J. Gomez-Tornero, D. Zelenchuk, G. Goussetis, and V. Fusco, "Substrate integrated waveguide leaky-wave antenna

designed for millimetre wave bands," *IET seminar on millimetre wave technologies for gigabit per second wireless communications,* 2012.

[113] M. Henry, C. E. Free, B. S. Izqueirdo, J. C. Batchelor, and P. Young, "Millimeter wave substrate integrated waveguide antennas: Design and fabrication analysis," *IEEE Trans. Adv. Pack.*, vol. 32, no. 1, pp. 93-100, Feb. 2009.

[114] W. Menzel, "Millimeter-wave radar for civil applications," *European Radar Conf.*, Paris, France, Sep. 2010, pp. 261-264.

[115] M. Lange and J. Detlefsen, "94 GHz three-dimensional imaging radar sensor for autonomous vehicles," *IEEE Trans. Microw. Theory Techn.*, vol. 39, no. 5, pp. 819-827, May 1991.

[116] S. Montusclat, F. Gianesello, D. Gloria, and S. Tedjini, "Silicon integrated antenna developments up to 80 GHz for millimeter wave wireless links," *European Conf. Wireless Technology*, Oct. 2005, pp. 237-240.

[117] J. A. G. Akkermans, M. H. A. J. Herben, and M. C. Van Beurden, "Balanced-fed planar antenna for millimeter-wave transceivers," *IEEE Trans. Antennas Propag.*, vol. 57, no. 10, pp. 2871-2881, Oct. 2009.

[118] J. Thornton, S. Gregson, and D. Gray, "Aperture blockage and truncation in scanning lens-reflector antennas," *IET Microwaves, Antennas & Propagation*, vol. 4, no. 7, pp. 828-836, July 2010.

[119] D. Deslandes and K. Wu, "Substrate integrated waveguide leaky-wave antenna: concept and design considerations," *Asia-Pacific Conference Proceedings*, Suzhou, China, Dec. 2005, pp. 346-349.

[120] A. J. Martinez-Ros, J. L. Gomez-Tornero, F. Quesada-Pereira, and A. Alvarez-Melcon, "Transverse resonance analysis of a planar leaky wave antenna with flexible control of the complex propagation constant," *IEEE International Symposium on Antennas and Propagation*, July 2011, pp.1289-1292.

[121] S. Paulotto, P. Baccarelli, F. Frezza, and D. R. Jackson, "Full-wave modal dispersion analysis and broadside optimization for a class of microstrip CRLH leaky-wave antennas," *IEEE Trans. Microw. Theory Techn.,* vol. 56, no. 12, pp. 2826-2837, Dec. 2008.

[122] W. C. Chew, *Waves and Fields in Inhomogeneous Media*, Piscataway NJ, Wiley/IEEE Press, 1995.

[123] P. Baccarelli, C. Di Nallo, S. Paulotto, and D. R. Jackson, "A full-wave numerical approach for modal analysis of 1-D periodic microstrip structures," *IEEE Trans. Microw. Theory Tech.*, vol. 54, no. 4, pp. 1350–1362, Apr. 2006.

[124] P. Baccarelli, P. Burghignoli, F. Frezza, A. Galli, P. Lampariello, G. Lovat, and S. Paulotto, "The nature of radiation from leaky waves on single- and double-negative metamaterial grounded slabs," *IEEE MTT-S International Microwave Symposium Digest*, vol.1, June 2004, pp.309-312.

[125] P. Baccarelli, P. Burghignoli, F. Frezza, A. Galli, P. Lampariello, G. Lovat, and S. Paulotto, "Fundamental modal properties of surface waves on metamaterial grounded slabs," *IEEE Trans. Microw. Theory Tech.*, vol. 53, no. 4, pp. 1431-1442, Apr. 2005.

[126] S. Paulotto, P. Baccarelli, F. Frezza, and D. R. Jackson, "Full-wave modal dispersion analysis and broadside optimization for a class of

microstrip CRLH leaky-wave antennas," *IEEE Trans. Microw. Theory Tech.*, vol. 56, no. 12, pp. 2826-2837.

[127] D. R. Jackson and A. A. Oliner, "A leaky-wave analysis of the high-gain printed antenna configuration," *IEEE Trans. Antennas Propag.*, vol.36, no.7, pp.905-910, July 1988.

[128] D. R. Jackson, A. A. Oliner, and A. Ip, "Leaky-wave propagation and radiation for a narrow-beam multiple-layer dielectric structure," *IEEE Trans. Antennas Propag.*, vol. 41, no. 3, pp. 344-348, March 1993.

[129] D. Nghiem, J. T. Williams, D. R. Jackson, and A. A. Oliner, "Existence of a leaky dominant mode on microstrip line with an isotropic substrate: theory and measurement," *IEEE MTT-S International Microwave Symposium Digest*, vol. 3, June 1993, pp.1291-1294.

[130] S. Paulotto, G. Valerio, D. R. Jackson, D. R. Wilton, P. Baccarelli, F. T. Celepcikay, W. A. Johnson, and A. Galli, "Efficient calculation of 1-D periodic Green's functions for leaky-wave applications," *Proceedings of URSI International Symposium on Electromagnetic Theory (EMTS)*, Berlin, Germany, Aug. 2010, pp. 204-207.

[131] W. A. Johnson, S. Paulotto, D. R. Jackson, D. R. Wilton, W. L. Langston, L. I. Basilio, P. Baccarelli, G. Valerio, and F. T. Celepcikay, "Modeling of general 1-D periodic leaky-wave antennas in layered media using EIGER™," *Proceedings of International Conference on Electromagnetics in Advanced Applications (ICEAA)*, Sydney, Australia, Sep. 2010, pp. 205-208.

[132] S. Otto, A. Rennings, T. Liebig, C. Caloz, and K. Solbach, "An energy-based circuit parameter extraction method for CRLH leaky-wave antennas," *Proceedings of the Fourth European Conference on Antennas and Propagation (EuCAP)*, Apr. 2010.

[133] M. A. Eberspächer and T. F. Eibert, "Analysis of composite right/left-handed unit cells based on even-odd-mode excitation," *IEEE Trans. Microw. Theory Tech.*, vol. 60, no. 5, pp. 1186-1196, May 2005.

[134] M. A. Eberspächer and T. F. Eibert, "Bloch mode analysis by even-odd-mode simulations," *Proceedings of the Seventh European Conference on Antennas and Propagation (EuCAP)*, Apr. 2013, pp. 1021-1023.

[135] G. Valerio, S. Paulotto, P. Baccarelli, P. Burghignoli, and A. Galli, "Accurate Bloch analysis of 1-D periodic lines through the simulation of truncated structures," *IEEE Trans. Antennas Propagat.*, vol. 59, no. 6, pp. 2188-2195, June 2011.

[136] J. Perruisseau-Carrier, K. Topalli, and T. Akin, "Low-loss Ku-band artificial transmission line with MEMS tuning capability," *IEEE Microw. Wireless Compon. Lett.*, vol. 19, no. 6, pp. 377-379, June 2009.

[137] J. Perruisseau-Carrier, A. K. Skrivervik, "Composite right/left-handed transmission line metamaterial phase shifters (MPS) in MMIC technology," *IEEE Trans. Microw. Theory Tech.*, vol. 54, no. 4, pp. 1582-1589, Apr. 2006.

[138] S. Paulotto, P. Baccarelli, and D.R. Jackson, "A self-matched wide scanning U-stub microstrip periodic leaky-wave antenna," *Journal of Electromagnetic Waves and Applications*, vol. 28, no. 2, pp. 151-164, 2014.

[139] J. R. James, P. Hall, and C. Wood, *Microstrip Antenna Theory and Design*, London, UK, Peter Peregrinus Ltd, 1981.

[140] S. Paulotto, P. Baccarelli, F. Frezza, and D. R. Jackson, "A novel technique for open-stopband suppression in 1-D periodic printed leaky-wave antennas," *IEEE Trans. Antennas Propagat.*, vol. 57, no. 7, pp. 1894-1906, July 2009.

[141] J. T. Williams, P. Baccarelli, S. Paulotto, and D. R. Jackson, "1-D combline leaky-wave antenna with the open-stopband suppressed: Design considerations and comparisons with measurements," *IEEE Trans. Antennas Propagat.*, vol. 61, no. 9, pp. 4484-4492, Sep. 2013.

[142] T. Liebig, S. Held, A. Rennings, and D. Erni, "Accurate parameter extraction of lossy composite right/left-handed (CRLH) transmission lines for planar antenna applications," *Proceedings of Fourth International Congress on Advanced Electromagnetic Materials in Microwaves and Optics*, Karlsruhe, Germany, Sep. 2010, pp. 456-458.

[143] M. J. Madou, *Fundamentals of Microfabrication: The Science of Miniaturization*, Third edition, Danvers MA, CRC Press, 2011.

[144] D. Chicherin, M. Sterner, D. Lioubtchenko, J. Oberhammer, and A. V. Räisänen, "Analogue type millimetre wave phase shifters based on MEMS tuneable high-impedance surface and dielectric rod waveguide," *International Journal of Microwave and Wireless Technologies*, vol. 3, no. 5, pp. 533-538, Oct. 2011.

[145] J. Hasch, E. Topak, R. Schnabel, T. Zwick, R. Weigel, and Ch. Waldschmidt, "Millimeter-wave technology for automotive radar sensors in the 77 GHz frequency band," *IEEE Trans. Microw. Theory Techn.*, vol. 60, no. 3, pp. 845-860, March 2002.

[146] M. Jensen and J.W. Wallance, "A review of antennas and propagation for MIMO wireless systems," *IEEE Trans. Antennas Propagat.*, vol. 52, no. 11, pp. 2810-2824, Nov. 2004.

Aalto-DD 190/2014

ISBN 978-952-60-5975-4 (printed)
ISBN 978-952-60-5976-1 (pdf)
ISSN-L 1799-4934
ISSN 1799-4934 (printed)
ISSN 1799-4942 (pdf)

Aalto University
School of Electrical Engineering
Department of Radio Science and Engineering
www.aalto.fi

BUSINESS + ECONOMY

ART + DESIGN + ARCHITECTURE

SCIENCE + TECHNOLOGY

CROSSOVER

DOCTORAL DISSERTATIONS